Ionic Currents in Single Isolated Bullfrog Atrial Cells

J. R. HUME and W. GILES

From the Department of Physiology and Biophysics, University of Texas Medical Branch, Galveston, Texas 77550

ABSTRACT Enzymatic dispersion has been used to yield single cells from segments of bullfrog atrium. Previous data (Hume and Giles, 1981) have shown that these individual cells are quiescent and have normal resting potentials and action potentials. The minimum DC space constant is ~920 μm. The major goals of the present study were: (*a*) to develop and refine techniques for making quantitative measurements of the transmembrane ionic currents, and (*b*) to identify the individual components of ionic current which generate different phases of the action potential. Initial voltage-clamp experiments made using a conventional two-microelectrode technique revealed a small tetrodotoxin (TTX)-insensitive inward current. The small size of this current ($2.5–3.0 \times 10^{-10}$ A) and the technical difficulty of the two-microelectrode experiments prompted the development of a one-microelectrode voltage-clamp technique which requires impalements using a low-resistance (0.5–2 MΩ) micropipette. Voltage-clamp experiments using this new technique in isolated single atrial cells reveal five distinct ionic currents: (*a*) a conventional transient Na^+ current, (*b*) a TTX-resistant transient inward current, carried mainly by Ca^{++}, (*c*) a component of persistent inward current, (*d*) a slowly developing outward K^+ current, and (*e*) an inwardly rectifying time-independent background current. The single suction micropipette technique appears well-suited for use in the quantitative study of ionic currents in these cardiac cells, and in other small cells having similar electrophysiological properties.

INTRODUCTION

Quantitative measurements of the magnitude and the time course of transmembrane ionic currents in cardiac muscle are limited by several inherent properties of most experimental preparations. For example, in ventricular and atrial trabeculae, as well as in isolated Purkinje fibers, the multicellular nature of the in vitro preparation gives rise to a number of significant technical and analytical problems: (*a*) significant axial and radial voltage decrements may be present, (*b*) ion accumulation or depletion may occur in small, "restricted"

Address reprint requests to Dr. Wayne R. Giles, Dept. of Physiology and Biophysics, University of Texas Medical Branch, Galveston, TX 77550. Dr. Hume's present address is Dept. of Pharmacology and Toxicology, School of Human Medicine, Michigan State University, East Lansing, MI 48824.

J. GEN. PHYSIOL. © The Rockefeller University Press · 0022-1295/83/02/0153/42 $1.00 153
Volume 81 February 1983 153–194

extracellular spaces, and (*c*) the three-dimensional intercellular coupling and restricted extracellular pathways constitute a significant access or series resistance that may be variable, even during a single experiment. The microanatomy and the cell size of some small multicellular preparations (rabbit and dog Purkinje fibers: Sommer and Johnson, 1968; Colatsky and Tsien, 1979*a*) might minimize these problems; nevertheless, they cannot be eliminated because of the inherent syncytial nature of cardiac muscle. As a result, a considerable effort has been directed toward developing techniques that may yield either viable isolated cardiac cells (Powell and Twist, 1976; Bustamonte et al., 1981) or clusters of cultured heart cells (Nathan and DeHaan, 1979; Ebihara et al., 1980), which are more suitable for electrophysiological studies. We have recently refined a simple technique for isolating single myocytes from bullfrog atrium. These isolated cells are relaxed and quiescent, and they retain the electrophysiological properties of cells within the intact atrium (Hume and Giles, 1981).

Our previous two-microelectrode analysis of the passive electrical properties of these single atrial cells showed that the minimum DC space constant (mean: 921 μm) of quiescent, relaxed cells that have recovered from a second electrode impalement is approximately four times the average length of a cell (mean: 204 μm). On this basis, we began a series of voltage-clamp experiments aimed at measuring each of the ionic currents underlying the action potential of single atrial cells. However, the conventional two-microelectrode approach involved a definite practical limitation: a very low success rate. We chose to study only those cells in which V_m was more negative than -80 mV after having "healed over" or recovered from the second impalement. The small diameter of the atrial cells and their ability to contract strongly when depolarized resulted in relatively few successful experiments, as well as severely limiting the recording time. These initial two-microelectrode voltage-clamp experiments did, however, reveal the presence of a small TTX-insensitive inward current. Moreover, these data indicated that the magnitude of this current, 3.23×10^{-10} A $\pm$ 47.5 (mean $\pm$ SE, $n = 6$) is sufficient to generate the observed maximum rate of depolarization of the slow response recorded in the presence of TTX (Giles and Hume, 1981).

The small magnitude of ionic currents in this preparation suggested that a single-microelectrode voltage-clamp technique may be applicable, provided that acceptable impalements could be made with a single low-resistance microelectrode. Such a method would *not* require rapid switching between current-passing and voltage-recording modes (cf. Merickel, 1980; Fishman, 1982) since the maximum voltage recording error arising from the series resistance of a 1-MΩ electrode that simultaneously measures voltage and passes 1 nA of current would be only 1 mV. In addition, a single-microelectrode clamp of this design would be expected to exhibit a relatively wide bandwidth because capacitative coupling, which may occur between a current-passing and a voltage-measuring electrode, would be eliminated.

In this paper, we describe a straightforward method of impaling single atrial cells with a low-resistance microelectrode (0.5–2.0 MΩ). Seal resistances

of several gigohms (10^9 Ω) are established routinely. This suction micropipette technique, in principle, is very similar to the one recently described by Hamill et al. (1981). We compare it with conventional microelectrode methods by making transmembrane potential measurements. The magnitude and voltage dependence of the TTX-resistant inward current recorded with this single-microelectrode voltage-clamp technique is compared and contrasted with data obtained using a conventional two-microelectrode method. In additional voltage-clamp experiments, this new technique is used to study i_{Na}, a time-independent (background) current, and a time-dependent K^+ current.

Some of these data have previously been reported in abstract form (Giles and Hume, 1981; Hume and Giles, 1982*a*, *b*).

METHODS

The enzymatic dispersion procedure for isolating single bullfrog atrial cells, the experimental chamber, and the optical apparatus used in this study were identical to those described previously (Hume and Giles, 1981).

Solutions and Drugs

Standard Ringer's solution was kept saturated with 95% O_2/5% CO_2 (pH 7.4) and contained (mM): 90.6 NaCl, 20 $NaHCO_3$, 2.5 KCl, 5.0 $MgCl_2$, 2.5 $CaCl_2$, and 10 glucose. When $[Ca^{++}]_o$ was varied, the total divalent cation concentration was held constant by adding or withdrawing $MgCl_2$.

In Na-free experiments, the solution was saturated with 100% O_2 and contained (mM): 2.5 KCl, 5.0 $MgCl_2$, 2.5 $CaCl_2$, 10 glucose, 5 HEPES, and 217 sucrose. The pH of this solution was titrated to 7.4 by adding NaOH. This produced a final Na^+ concentration of 1–2 mM. TTX was purchased from Sigma Chemical Co., St. Louis, MO; $CdCl_2$ was purchased from Aldrich Chemical Co., Inc., Milwaukee, WI. HEPES buffering was used in all Cd^{++}-containing Ringers.

Microelectrode Fabrication

Originally we planned to voltage-clamp and internally perfuse single atrial cells by using the recently developed suction pipette technique (Lee et al., 1980). However, the diameter of single frog atrial cells (4–7 μm) is much smaller than the diameter of rat ventricular myocytes (10–35 μm; Powell and Twist, 1976); therefore, it was necessary to construct suction pipettes with tip sizes much smaller than those (10–15 μm) used by Lee et al. (1980). The fabrication of acceptable pipettes having these very small tip diameters is rather difficult. Moreover, even if such pipettes can be made, their small tip size might compromise one important advantage of this approach: the ability to internally perfuse quickly and effectively. Therefore, the technique we use is a hybrid suction pipette method in which negative pressure is applied to low-resistance microelectrodes in order to establish a high-resistance seal and then rupture the sarcolemma, thereby forming a low-resistance pathway to the interior of the cell. No attempt has yet been made to assess whether effective internal perfusion can be accomplished with these small tip diameter microelectrodes.

For negative pressure to be transmitted effectively to the tip of a microelectrode, its shank must be relatively short (3–5 μm). This was accomplished by using a single-turn heater coil on a vertical pipette puller (David Kopf Instruments, Tujunga, CA). Microelectrodes were selected which, when filled with 3 M KCl, had resistances ranging from 0.5 to 2.0 MΩ. The use of conventional fiber-filled microelectrode glass

tubing simplifies filling the electrodes with 3 M KCl. However, the fiber often occludes the tip and prevents the transmission of negative pressure through it. The use of Radnoti Glass Technology, Inc., (Monrovia, CA) microstar capillary tubing (1.0 mm OD) proved to be preferable because it has no fiber in the shank, but can be back-filled very readily. The KCl electrolyte solution was filtered through a membrane filter (0.45 μm pore size) before use.

Experimental Procedure

The low-resistance microelectrodes are mounted in a microelectrode holder that has a suction port (EH-900R; W-P Instruments, Inc., New Haven, CT). A 2-ft length of polyethylene tubing (0.032 in ID) is connected from the suction port of the microelectrode holder to a 1-ml syringe (Hamilton 1001; A-M Systems, Toledo, OH), which is used to produce graded negative pressure. The microelectrode holder is carefully back-filled with 3 M KCl to ensure that no bubbles remain in the shank. The holder is then connected to a preamplifier (KS-700; W-P Instruments, Inc.), the headstage of which is mounted on the stage of an inverted microscope (Swift Instruments Ltd., San Jose, CA).

Under magnification of 600, the microelectrode tip is very gently pressed against the sarcolemma of an isolated atrial cell. A sudden pulse of negative pressure is then applied using a valve connected to the syringe. After 10–30 s a very high seal resistance (several gigohms) is usually established. Typically, this sealing is followed by a rupture of the membrane, which is indicated by a rapid voltage deflection to −80 or −90 mV, i.e., to the resting potential of a quiescent atrial cell. The negative pressure gradient is critical: if too much suction is applied, the cell will undergo irreversible contracture, but too little suction will fail to rupture the membrane. We have found that each microelectrode can be used only once, as is the case for the patch pipettes used to record single-channel currents (Neher et al., 1978).

The recent literature has included a number of interesting discussions of the possibility that there may be a significant leakage of K^+ from conventional microelectrodes filled with 3 M KCl (cf. Fromm and Schultz, 1981). This may be caused by electrodiffusion and/or the hydrostatic pressure of the fluid-filled electrode shank, and it may be as large as 2.0×10^{-14} mol/s for a 16–30-MΩ electrode. Two of our consistent findings rule out any significant net K^+ gain by impaled single atrial cells. (*a*) The reversal potential for the slow outward current (see Results) is very near the calculated E_k (see also *Outward Current*), and it remains stable for periods during which a series of voltage-clamp depolarizations are applied. (*b*) Stable resting potentials are measured in the cells for periods of at least 30 min.

Thus, it appears that the constant application of suction to the shank of our microelectrodes markedly reduces leakage of the electrolyte from the tip. However, relatively large membrane potential artefacts, about −15 mV, are observed in some impalements. Although the basis for this standing potential has not been investigated systematically; it may arise from either (*a*) Ringers fluid being sucked into the tip of the microelectrode, or (*b*) a patch of sarcolemma moving into the electrode tip, thus displacing a tiny amount of 3 M KCl.

Enzymatically isolated single atrial cells have a relatively high input resistance (average of 220 MΩ determined with conventional microelectrodes; Hume and Giles, 1981); hence the ability to record "normal" resting membrane potentials with these low-resistance microelectrodes provides some evidence that large seal resistances are produced by the suction method. To measure the seal resistance, a series of experiments was done in which the microelectrode was connected to the input of a current-to-voltage amplifier. The seal resistances achieved before rupture of the atrial cell

membrane averaged 12.9 GΩ (±5.1 SE, $n = 8$). A direct comparison has been made of resting potentials and action potential parameters recorded with both the new suction microelectrode method and a previous conventional microelectrode technique. These data are presented in Table I, which demonstrates that there are no significant differences between the two techniques. The slightly higher value of R_{in} measured with suction microelectrode might be due to the higher seal resistance consistently obtained when using it as opposed to conventional microelectrodes.

Series Resistance (R_s) Determination

The equivalent circuit for our suction microelectrode is similar to that previously described for the suction pipette (Lee et al., 1980). The ability to use a single suction pipette or microelectrode to measure voltage and pass current simultaneously depends critically upon the magnitudes of (*a*) the total resistive pathway in series with the membrane resistance and (*b*) the magnitude of current flow. An upper limit of the series resistance in these experiments can be obtained by summing the maximum resistance of the microelectrode (2 MΩ) and the 1-MΩ resistor used to measure current, i.e., the resistor placed between the microelectrode and the amplifier input

TABLE I

ELECTRICAL PROPERTIES OF FROG ATRIAL CELLS

	Conventional microelectrodes ($n = 12$)*	Suction microelectrodes ($n = 8$)‡
Resting membrane potential	−88.6±1.7 mV	−89.6±1.2 mV
Action potential amplitude	124.4±8.1 mV	131.6±2.6 mV
Action potential duration	722.5±106.3 ms	772.5±43.4 ms
Input resistance (R_{in})	219.8±77.4 MΩ	283.9±56.8 MΩ
Membrane time constant (τ_m)	19.7±7.3 ms	23.1±4.0 ms

* From Hume and Giles, 1981. Mean ± SD.

‡ Mean ± SD.

stage (see Fig. 2 below). If the peak of current flow under voltage-clamp conditions is 6.0×10^{-10} A, a maximum error of 1.8 mV will result. Horn and Brodwick (1980) have recently pointed out that in the case of macroscopic suction pipettes (10–20 μm ID) the pipette resistance can increase dramatically after application of negative pressure. This has been attributed to the tip becoming partly occluded by cytoplasmic material. To determine whether our micropipette resistance shows a similar increase after application of negative pressure, tests such as that illustrated in Fig. 1 were carried out in a number of cells.

After a gigohm seal was established and rupture of the membrane occurred, relatively large hyperpolarizing current pulses were applied to measure the total R_s, manifested as the instantaneous voltage change. In the experiment shown in Fig. 1, an instantaneous voltage drop of 1.2 mV was detected (see inset). The microelectrode resistance in this trial was 1.8 MΩ and a 1-MΩ fixed resistor was used to measure current. The voltage drop across an R_s of 2.8 MΩ produced by a current of 4.0×10^{-10} A would be 1.1 mV. Therefore, some increase in R_s did occur after establishment of the seal; however, it was very small (see also Table II). In summary, the voltage drop across the total series resistance appears to be negligible, provided that the current flow is less than 1×10^{-9} A.

Voltage Clamp

A block diagram of the potential recording and voltage-clamp circuits is shown in Fig. 2. The voltage signal from the suction micropipette was led to the (−) side of a FET input unity gain amplifier (KS-700; W-P Instruments, Inc.). As pointed out previously (Hume and Giles, 1981), the rather large input resistance of the isolated atrial myocytes (200–300 MΩ) makes it essential to null completely the leakage

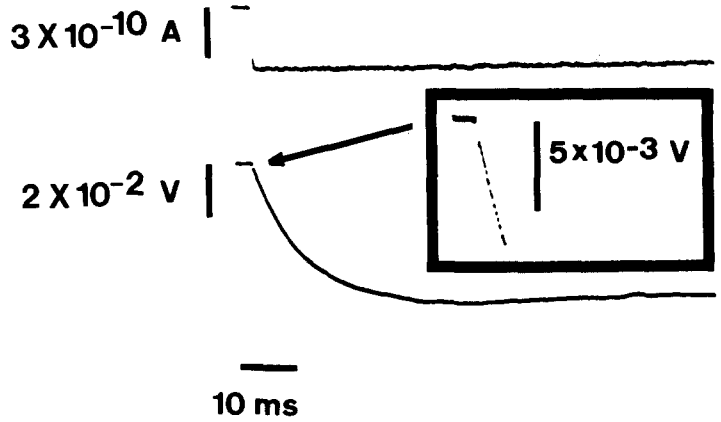

FIGURE 1. Measurement of the series resistance (R_s) after establishment of a gigohm seal with a suction microelectrode. A large hyperpolarization from the resting potential was elicited by intracellular injection of inward current through the suction microelectrode. The small instantaneous voltage jump (see inset) at the ON is due to a voltage drop across R_s (see text for further explanation).

TABLE II

COMPARISON OF TOTAL SERIES RESISTANCE (R_s) WITH MICROPIPETTE RESISTANCE (R_e)

Preparation	R_s	R_e*
	MΩ	*MΩ*
12-15-81-1	3.3	3.0
12-15-81-2	3.7	2.8
12-15-81-3	3.1	2.8
12-16-81-7	2.9	2.8
12-18-81-2	3.5	2.2
12-18-81-3	2.4	2.1
12-18-81-4	3.0	3.0
Mean =	3.13±0.16 (SE)	2.67±0.14 (SE)

* R_e is the sum of the micropipette resistance and a 1-MΩ fixed resistor that was used to measure current.

current of this amplifier at regular intervals. The membrane potential signal, $-V_m$, was then compared with the rectangular command voltage level using a differential amplifier (AM 502; Tektronix Inc., Beaverton, OR) having variable gain and bandwidth. Typically, this feedback amplifier was run at a gain of 300 with a bandwidth of DC–3 kHz. The error signal was applied to the suction micropipette via the current-passing section (denoted S) of the KS-700. The rectangular pulses were

generated by applying the TTL pulses from a digital clock (W-P Instruments, Inc.) to a voltage divider circuit, which had an optical isolation unit at its output. The holding potential was varied by applying a 5-V DC level to a second voltage divider circuit.

Membrane current was monitored in two ways. Initially, it was collected in the superfusion chamber using an Ag/AgCl pellet connected to a conventional operational amplifier circuit arranged as a current-to-voltage converter. Later, and in the majority of the experiments illustrated in this paper, current was measured as the voltage drop across a 1-MΩ resistor positioned at the output of the feedback amplifier. The differential amplifier used for this purpose was designed and constructed by Dr. T.

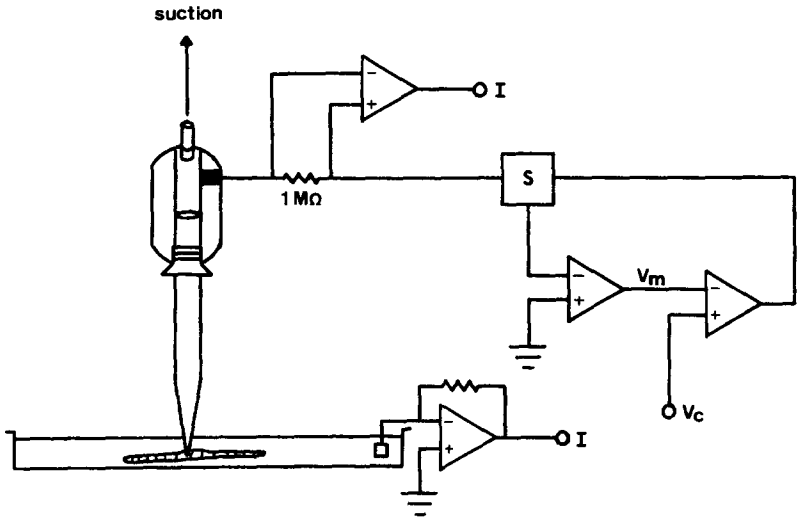

FIGURE 2. Experimental setup for single suction microelectrode voltage clamp. Diagram illustrates a single atrial cell attached to a suction microelectrode. The potential (V_m) was monitored using a KS-700 microprobe system (W-P Instruments, Inc.). The rectangular box denoted S is a port on the KS-700 that permits current injection through the high-impedance probe. Note that current can be measured in two different ways: (*a*) by collecting it in the superfusion chamber, or (*b*) as the ΔV across a 1-MΩ resistor placed at the output of the voltage-clamp amplifier.

Iwazumi, University of Texas, Galveston, TX. It has very low input capacitance (±1 × 10^{-13} F) and a bandwidth of DC–100 kHz. Both methods of current measurement gave similar results; however, the latter method significantly improved the signal-to-noise ratio. A virtual ground circuit (model 180; W-P Instruments, Inc.) was used to stabilize the bath potential.

Membrane potential and current signals were monitored using a storage oscilloscope and recorded continuously on an FM tape recorder (model 3964; Hewlett-Packard, Co., San Diego, CA) operated at a bandwidth of DC–5 kHz. Data analysis was done off-line by replaying the recorded data into either a storage oscilloscope or a pressurized ink pen recorder (model 440; Gould-Brush Instruments, Cleveland, OH). For analysis of capacitative transients, membrane potential and current measurements were recorded on an FM tape recorder (model 4DS; Racal Recorders Inc.,

Covina, CA) at a bandwidth of DC–20 kHz. Subsequent off-line analysis was done with a digital processing oscilloscope (model 3001; Norland Corp., Fort Atkinson, WI).

In certain experiments, series resistance compensation was necessary. The original method of Hodgkin et al. (1952) was implemented by adding part of the signal from the current-to-voltage converter to the command voltage. In addition, we incorporated a suggestion of Sigworth (1980), which greatly improves the clamp stability when R_s compensation is used. This involves filtering the current monitor signal at a high frequency in order to minimize phase mismatches within the feedback loop. In our experiments, an eighth-order Butterworth filter was set at 25 kHz. This means that the series resistance is compensated effectively at times longer than ~40 μs after the "make or break" of a command clamp pulse.

RESULTS

Membrane Capacitance

The membrane capacitance of single frog atrial cells was studied using both one- and two-microelectrode voltage-clamp techniques. Fig. 3A illustrates the surge of capacitative current flow in response to a 20-mV depolarizing voltage-clamp step obtained with the one-microelectrode voltage-clamp method. A peak magnitude of $\sim 6 \times 10^{-9}$ A is reached within 60 μs; the current then decays with single exponential time course (panel C) having a time constant of ~200 μs.

Previous double sucrose gap voltage-clamp measurements of the capacitative transient (i_{cap}) in bullfrog atrial trabeculae have yielded variable and conflicting results. Rougier et al. (1968) originally reported that i_{cap} decayed with a single exponential time course that varied widely (0.2–5.9 ms). Tarr and Trank (1971) also found the decay of i_{cap} to be a single exponential, but their data yielded a τ of ~1 ms. Connor et al. (1975) later showed that the time course of the decay of i_{cap} in frog atrium is best described as the sum of two or three exponentials having τ's ranging from 0.13 to 4.2 ms.

The relatively fast rate of decay of the capacitative transients recorded from single atrial cells may be attributed to a significant reduction in the series resistance. A large series resistance arising from, e.g., endothelial layers of tissue and/or intercellular clefts in multicellular preparations (see Attwell and Cohen, 1977) would be expected to slow the decay of the capacitative transient. The single exponential time course of decay of i_{cap} implies that a single atrial cell can be modeled as a simple parallel RC network. This equivalent circuit is consistent with the previous anatomical studies which have shown that the T system is sparse or absent in frog heart cells (Barr et al., 1965; Sommer and Johnson, 1969; Page and Niedergerke, 1972).

The total capacitance of a single atrial cell and the specific membrane capacitance can be obtained from the integral of the capacitative currents and the membrane surface area. The total capacitance of a single atrial cell obtained using the one-microelectrode voltage-clamp method was calculated to be 7.6×10^{-11} F (± 0.5 SE, $n = 5$). Assuming single atrial cells to have a cylindrical geometry ($d = 5$ μm; $l = 190$–220 μm), the calculated surface areas

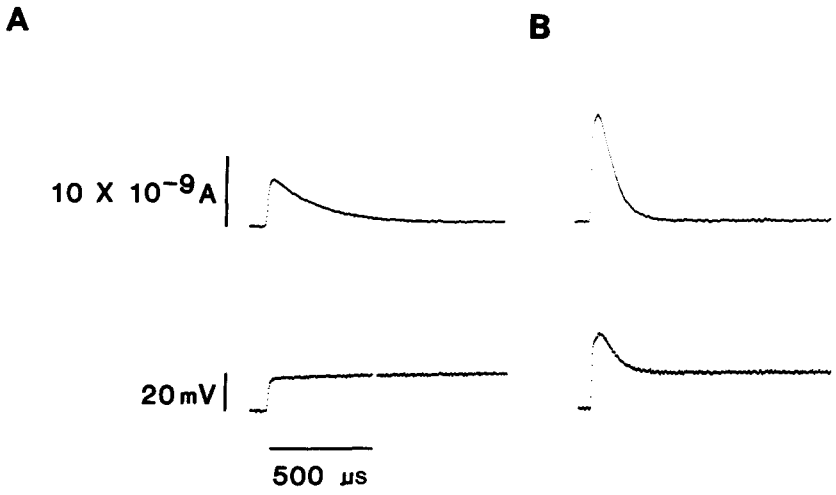

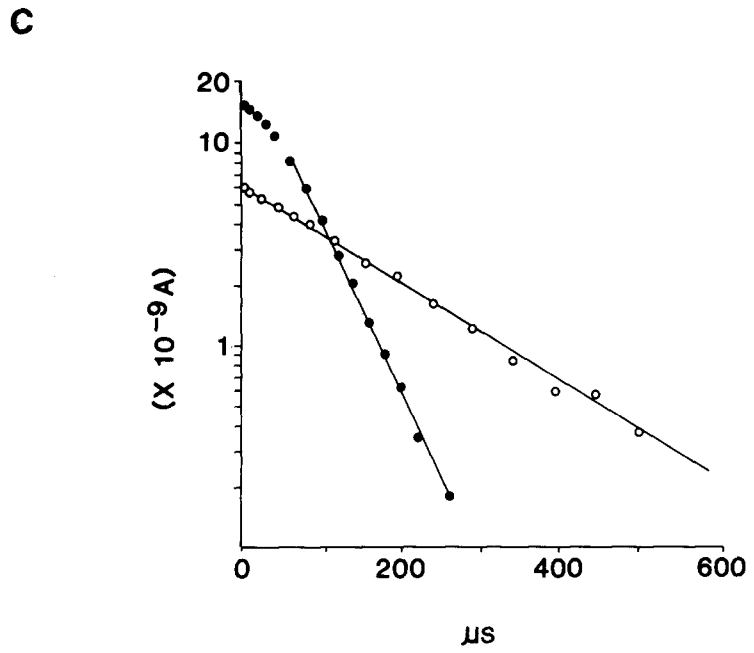

FIGURE 3. Capacitative currents elicited by depolarizing voltage-clamp steps without (A) and with (B) series resistance compensation. The time course of decay of each of these capacitative transients is plotted below (panel C) using log i_{cap} vs. time coordinates. The time constant of decay of i_{cap} was 200 μs (○, before) and 80 μs (●, after R_s compensation).

range from 3.0 to 3.5 × 10^{-5} cm^2, and the resulting specific membrane capacitance is 2.3 $\mu F/cm^2$ (± 0.2 SE, $n = 5$). Identical experimental protocols, using a two-microelectrode voltage-clamp method, yielded a total membrane capacitance of 7.6 × 10^{-11} F (± 0.9 SE, $n = 5$) and a specific membrane capacitance of 2.4 $\mu F/cm^2$ (± 0.3 SE, $n = 5$). Hence, both voltage-clamp methods yielded similar values for the total and the specific membrane capacitance.

These values of the specific membrane capacitance are also quite similar to those estimated previously from our two-microelectrode study of the decay of electrotonic potentials (2.2 $\mu F/cm^2$; Hume and Giles, 1981). However, all of these estimates are based upon surface area calculations which assume a simple right cylinder geometry of the cell and hence neglect any contribution of surface caveoli to the total membrane surface area. If these surface caveoli increase the total surface area by 50% (Masson-Pevet et al., 1980), then the specific membrane capacitance is ~1.5 $\mu F/cm^2$, a value within the accepted range of most biological membranes (Cole, 1968).

Careful comparison of the time course of (*a*) the approach of i_{cap} to the baseline and (*b*) the settling time of the clamp step can provide information regarding the presence and magnitude of the total series resistance. The data obtained from atrial trabeculae (Rougier et al., 1968; Tarr and Trank, 1971) showed quite clearly that i_{cap} did not decay completely until 1–2 ms after the clamp step had reached a constant value, which indicates that the series resistance is appreciable in these preparations. From our data in Fig. 3A, it is apparent that the decay of i_{cap} does "lag" the settling of the voltage step, which suggests that a significant resistance is in series with the membrane resistance.

If the decay of i_{cap} is limited only by the resistance to longitudinal current flow (R_i) within the cell, it is possible to estimate the time constant of decay of i_{cap} using the approach of Schoenberg et al. (1975). The final time constant of decay of i_{cap} for a voltage step in a RC cable with sealed ends is given by:

$$\tau_o = \frac{\tau_m}{1 + (\pi^2/4)\,(\lambda/h)^2}. \quad (1)$$

λ is the longitudinal space constant and h is 0.5 of the cell length. Using our (Hume and Giles, 1981) previously determined values for τ_m (19.7 ms) and λ (921 μm), τ_o should be ~95 μs, or about twice as fast as that observed.

The major portion of the series resistance is probably due to the micropipette resistance, when a single pipette is used to pass current and simultaneously monitor transmembrane potential. To test this, we determined the total series resistance from the capacitative transients ($R_s = \Delta V_m/\Delta I_{peak}$; Connor et al., 1975) and compared these values with the micropipette resistances that were measured before attaching to the cell. Such a comparison was made in seven cells; these results are summarized in Table II. The mean value of the total series resistance determined from the capacitative transients was ~20% greater than the mean value of the combined micropipette resistance and the 1-MΩ fixed resistor. This may indicate either that the additional 500-kΩ resistance

is intrinsic to the preparation and bath, or that there is a small increase in the pipette tip resistance after attachment to the cell surface, coincident with formation of the giga-seal. When expressed in terms of the cell surface area, this resistance is 23 Ωcm^2. For comparison, measurements of R_s in multicellular cardiac preparations yield values ranging from 200 to 600 Ωcm^2 (Beeler and Reuter, 1970; New and Trautwein, 1972).

Although relatively low-resistance micropipettes (0.5–2.0 MΩ) can be used in these experiments, a shortcoming of the single-electrode clamp method is the slowing of the capacity transients caused by the micropipette tip resistance. This becomes more pronounced for larger voltage-clamp steps and may prevent quantitative analysis of ionic currents with rapid activation kinetics. It was important therefore to determine whether most of the series resistance arising from the micropipette tip could be effectively nulled with series resistance compensation. Fig. 3B shows the time course of the capacitative transient recorded from a cell using compensated feedback. Compensating for R_s increases the peak amplitude of i_{cap} and accelerates its rate of decay. The rate of decay of i_{cap} when R_s is compensated is close to that expected if the decay of i_{cap} is limited only by the intracellular resistance. It is usually not possible to achieve faster transients than those shown in Fig. 3B, because when compensated feedback is used, the feedback loop is prone to oscillation, which immediately causes cell death. In summary, these results suggest that compensated feedback can significantly reduce the contribution of the micropipette tip resistance to the total series resistance. When a command voltage step is applied, this compensation shortens the time needed for the transmembrane voltage to be clamped to the new potential.

Two Transient Inward Currents

Previous experiments using standard microelectrode techniques have established that in single bullfrog atrial cells, two types of regenerative response can be elicited by intracellular stimulation (Hume and Giles, 1981). In normal Ringers solution, action potentials with a maximum rate of depolarization ($\dot{V}_{max}$) of ~40 V/s are typically recorded. After addition of micromolar concentrations of TTX, action potentials of similar magnitude and duration can be elicited; however, the maximum rate of depolarization of these slow responses is reduced to ~2 V/s. Our initial voltage-clamp experiments were aimed at investigating the nature of the transient inward currents underlying these responses in single atrial cells. Both the one-microelectrode voltage clamp and a conventional two-microelectrode clamp technique were used.

Examples of the two types of regenerative responses that can be elicited in single atrial myocytes are illustrated in Fig. 4A. A sequence of six elicited action potentials is shown: the first action potential was obtained before addition of TTX and the remaining five were obtained during the wash-in of 30 μM TTX. In this cell, TTX slowed the maximum rate of depolarization, reduced the overshoot, and prolonged the action potential duration. The action potential recorded before TTX and the final action potential recorded in 30 μM TTX are similar to fast and slow responses which have been recorded

in a variety of multicellular cardiac preparations (see Reuter, 1979; Carmeliet and Vereecke, 1979, for review).

Panel B shows data from an analogous experiment performed under voltage-clamp conditions in another cell. The cell was clamped to −90 mV (near the resting potential) and six voltage-clamp steps to 0 mV were applied before and during the wash-in of 30 μM TTX. Before the addition of TTX, a rapidly activating inward current which peaked within ~1 ms and turned off within

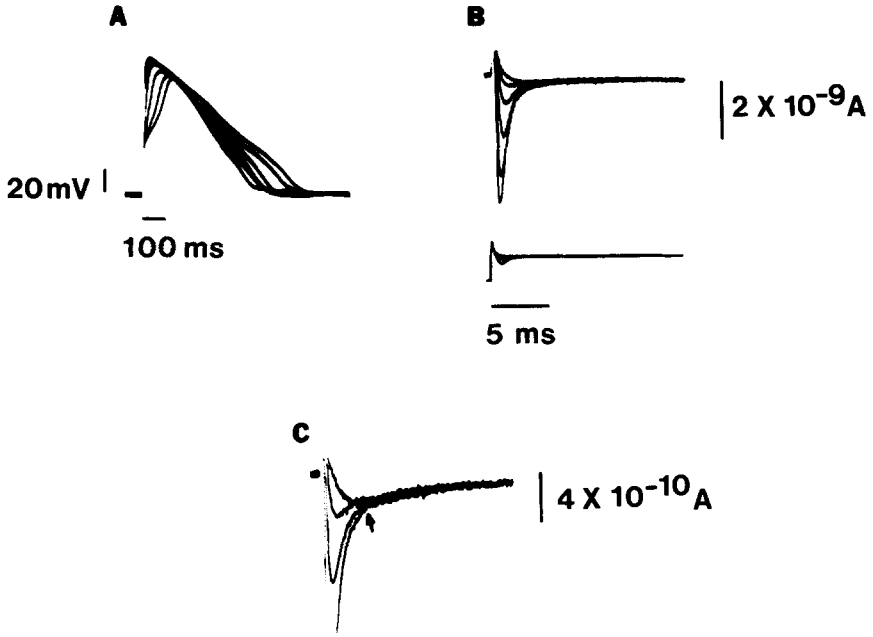

FIGURE 4. Action potentials and the underlying inward currents in single isolated bullfrog atrial cells. Panel A shows an action potential elicited in standard Ringers solution; the five additional action potentials that are superimposed were obtained after starting the superfusion of 3.0×10^{-5} M TTX. Panel B shows the effects of the same dose of TTX under voltage-clamp conditions. Repetitive 90-mV voltage-clamp steps from a holding potential of −90-mV were applied immediately after starting the superfusion of TTX (the largest transient inward current was elicited prior to TTX superfusion). Panel C shows the same currents as in B at a higher gain. R_s compensation and the single suction micropipette voltage clamp were used. The stimuli and clamp pulses were applied at 0.25 Hz.

5 ms was observed. The peak magnitude of this fast inward transient current was 4.2×10^{-9} A. During the wash-in of 30 μM TTX, the magnitude of the transient fast inward current progressively declined; thus, the sixth voltage-clamp pulse apparently failed to elicit an inward current. However, when the gain of the current trace was increased (panel C), the presence of a small, TTX-insensitive transient inward current was revealed (indicated by arrow). This inward current was consistently observed even after long-term (several

hours) application of TTX. In the cell shown in Fig. 4C, this TTX-insensitive inward current reached its peak value within 4 ms at an amplitude of 2.2×10^{-10} A. It then turned off with a much slower time course than the larger and faster transient inward current. The presence of these two pharmacologically distinct transient inward currents has been observed consistently and confirms earlier findings in frog atrial trabeculae (Rougier et al., 1969; Tarr and Trank, 1971).

The data in Fig. 4 may be indicative of use-dependent block of i_{Na} by TTX. This phenomenon has been described recently in multicellular cardiac preparations (Baer et al., 1976; Cohen et al., 1981). However, this possibility will have to be carefully re-assessed under conditions in which the time course of equilibration of the toxin within the experimental chamber is controlled systematically.

Sodium Inward Current

The sensitivity to TTX and kinetics of the fast transient current suggest that it is a sodium current, similar to that previously studied in intact frog atrium (Haas et al., 1971). A series of experiments were carried out to assess the usefulness of a single-micropipette voltage clamp for studying the fast inward sodium current. In principle, the single atrial cell preparation offers several advantages for studying i_{Na}. (*a*) The absence of an extensive T system is likely to minimize the possibility of any significant radial voltage inhomogeneity. (*b*) The relatively slow rate of depolarization of the action potential (40 V/s) indicates that the peak inward sodium current may be relatively small, even in normal extracellular sodium.

Despite these advantages, however, the single-microelectrode voltage clamp may be limited by a series resistance error, since in normal Ringers i_{Na} is 3–6 nA in size. The pipette resistances ranged from 0.5 to 2.0 MΩ; hence, the voltage error during the flow of such Na^+ currents will be significant. To assess the extent of this series resistance error, we have compared the kinetics and voltage dependence of i_{Na} using the single-microelectrode clamp with and without compensated feedback. Fig. 5 shows the results of one such experiment. $CdCl_2$ (10^{-3} M) was used to block the TTX-insensitive inward current (see *TTX-insensitive Inward Current* below). The left panel shows i_{Na} elicited by progressive voltage clamp steps to −57, −35, and +5 mV from a holding potential of −95 mV in normal Ringers solution. The time to peak of i_{Na} gets faster as the cell is clamped to more positive potentials. However, the relatively slow settling of the capactitative transient is also evident in the absence of compensated feedback. From the voltage traces corresponding to these currents, it is apparent that during the large surge of i_{cap}, the voltage is not constant. At the peak of i_{Na} on the second step, there is a clear inflection of the voltage trace, which indicates some loss of control.

The current and voltage traces in the right panel of Fig. 5 were obtained in the same cell using compensated feedback. Identical voltage-clamp steps to −57, −35, and +5 mV elicited significantly *larger* sodium currents with a much faster time to peak. It is also clear that the decay of i_{cap} is speeded considerably, being complete within 400 μs. The lower traces show the

corresponding voltage steps associated with each of the currents. Note that the positive feedback occurring during the surge of the capacitative transients and peak inward currents is added to the rectangular command pulse, resulting in the hump in the voltage trace ($V_{R_s} + V_m$). This direct comparison of the currents obtained before and after implementation of compensated feedback indicates that the series resistance caused by the micropipette tip can significantly slow the kinetics and attenuate the amplitude of i_{Na}.

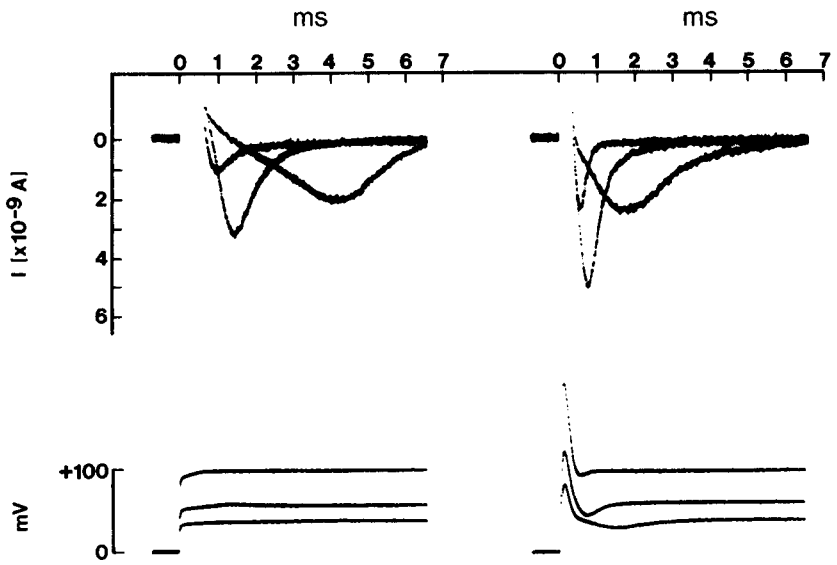

FIGURE 5. Comparison of magnitude and time course of i_{Na} elicited by three voltage-clamp depolarizations with (right side) and without (left side) R_s compensation. Top traces are currents and the bottom traces are command voltages. Records obtained in the same cell in response to clamp depolarizations to −57, −35, and +5 mV. $CdCl_2$ (10^{-3} M) was present throughout. Holding potential: −95 mV.

In Fig. 6 the current-voltage relation of the peak inward current in this experiment is plotted. The open circles indicate data obtained without compensated feedback. The peak inward current occurred near −50 mV at an amplitude of 3.2×10^{-9} A. There is a clear asymmetry in the voltage dependence, which is probably indicative of poor voltage control caused by the presence of a large series resistance (Taylor et al., 1960; Jack et al., 1975). When series resistance compensation is used (filled circles), the peak of the *I-V* relation is increased to 5.2×10^{-9} A and is shifted ~20 mV to the right. In addition, series resistance compensation makes the peak inward current-voltage relation for i_{Na} much more symmetrical. It would appear therefore that the major effects of the series resistance (which is largely attributable to the pipette resistance) are a slowing of the kinetics, a distortion of the voltage dependence, and an attenuation of the amplitude of i_{Na}.

To assess whether the peak inward current-voltage relation of i_{Na} obtained using compensated feedback accurately reflects the voltage dependence of i_{Na}, a series of experiments was carried out using partially blocking doses of TTX to reduce the magnitude of i_{Na}. An interesting consistent finding is that the Na^+ current of single frog atrial cells has approximately the same sensitivity to TTX as found in nerve (Narahashi et al., 1964). This high sensitivity to TTX is unusual for Na^+ channels in heart (Dudel et al., 1967; Narahashi, 1974; Baer et al., 1976; Cohen et al., 1979). However, a relatively high sensitivity to TTX has previously been observed in intact frog atrial trabeculae (Tarr and Trank, 1974; Connor et al., 1975). In addition, Tanaka and Barr (1982) have reported that a frog myocardial sarcolemma preparation has a

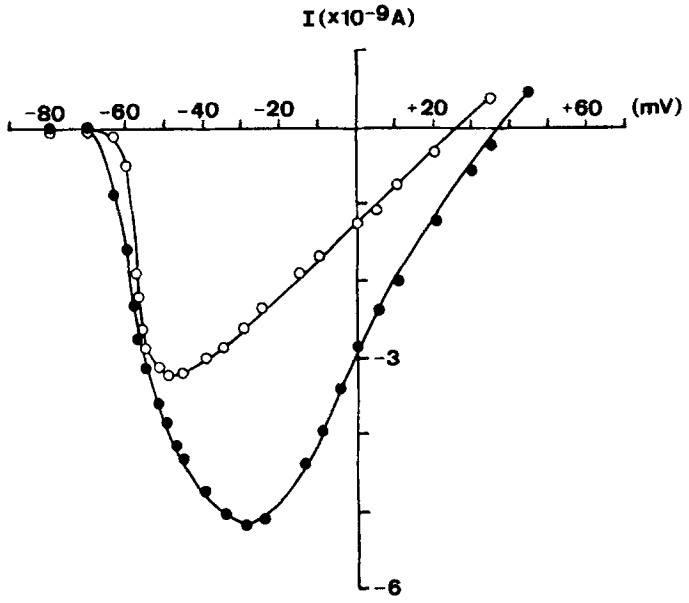

FIGURE 6. Effect of R_s compensation on the peak inward current-voltage relation of i_{Na}. Open circles indicate data obtained without R_s compensation; filled circles show data obtained after R_s compensation. Currents are from the same cell as in Fig. 5 under identical conditions (1×10^{-3} M $CdCl_2$).

high affinity binding site for saxitoxin ($K_D \sim 10^{-8}$ M). Therefore, the high sensitivity of single atrial cells to TTX is not necessarily surprising; it may indicate that the enzymatic dispersion procedure does not modify the sodium channel. A high sensitivity to TTX has also been found in the chick embryonic heart (Iijima and Pappano, 1979).

Fig. 7 shows a peak inward current-voltage relation obtained without compensated feedback in the presence of 3×10^{-8} M TTX and 1×10^{-4} M $CdCl_2$. This concentration of TTX reduced the peak magnitude of i_{Na} by ~10-fold. Peak inward current is first detected near −60 mV and it reaches a maximum ($\sim 4.0 \times 10^{-10}$ A) near −25 mV. The apparent reversal potential is

near +35 mV. The *I-V* curve is quite symmetrical, which suggests adequate clamp control over the entire range of activation. Comparison of the data obtained in normal $[Na^+]_o$ using compensated feedback with that in which i_{Na} was reduced to 10% of its control values reveals definite similarities in (*a*) the shape of the *I-V* relation, (*b*) the potential at which the peak i_{Na} was recorded, and (*c*) the apparent reversal potential of i_{Na}. These data suggest strongly that voltage recording errors arising from the series resistance of the

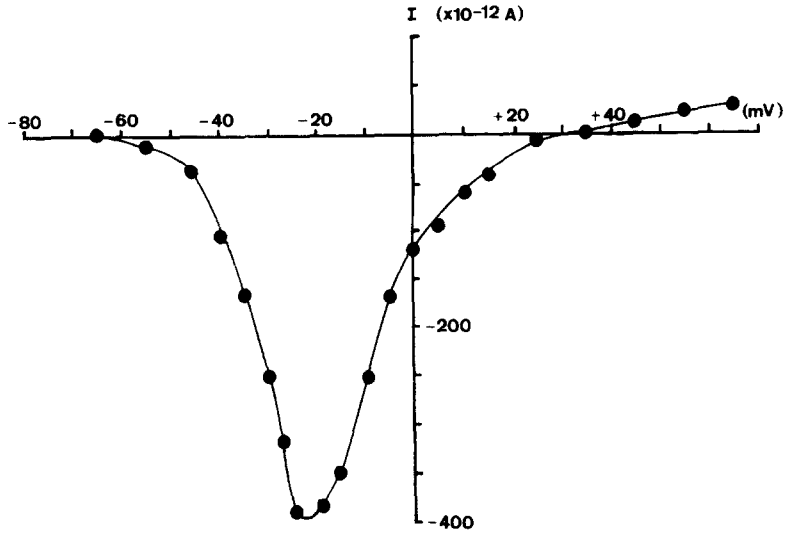

FIGURE 7. Peak inward current-voltage relation for i_{Na} in the presence of a dose of TTX (3×10^{-8} M) that reduced i_{Na} by ~90%. No R_s compensation was used in this experiment. 10^{-4} M $CdCl_2$ was used to block i_{Ca}^{++}. Holding potential: −85 mV.

pipette tip can be minimized by compensated feedback and/or by reducing the size of i_{Na}.

One test that assesses the adequacy of voltage control during activation of a fast transient current (e.g., i_{Na}) is to terminate the voltage-clamp step near the peak of its activation (Harrington and Johnson, 1973; Colatsky and Tsien, 1979*b*; Brown et al., 1981). Fig. 8 illustrates this type of experiment under compensated feedback conditions. From a holding potential of −90 mV, three voltage-clamp steps to −30 mV were applied for durations of 0.85, 1.5, and 1.9 ms. The current tails immediately following repolarization to −90 mV exhibit a smooth and rapid decay: i_{cap} merges with the tail currents of i_{Na}, which appear to decline in amplitude as the duration of the voltage pulse is increased. These results suggest that adequate voltage control can be achieved even during the peak sodium current, provided that compensated feedback is used to overcome the influence of the pipette tip resistance. A complete "envelope of tails" experiment for i_{Na} has not yet been attempted. This will be done in conjunction with a more detailed study of i_{Na}.

It should be noted, however, that none of the above tests establishes unequivocally that the single atrial cell is space clamped during the activation

of i_{Na} in normal $[Na^+]_o$. Inspection of Table I in conjunction with the data obtained using compensated feedback shown in Fig. 7 yields the following data. The average input resistance, measured with one microelectrode, of an atrial cell is ~300 MΩ, giving a minimum DC space constant of 1,008 μm. The slope resistance of the i_{Na} *I-V*, measured between 0 mV and the apparent reversal potential, drops to 14 MΩ. Since the space constant is proportional to $\sqrt{R_m}$, this means that the minimum active DC space constant is ~215 μm, or 1 cell length. In summary, although the i_{Na} data recorded in 100% $[Na^+]_o$ meet a number of criteria for adequate space clamping, caution should be

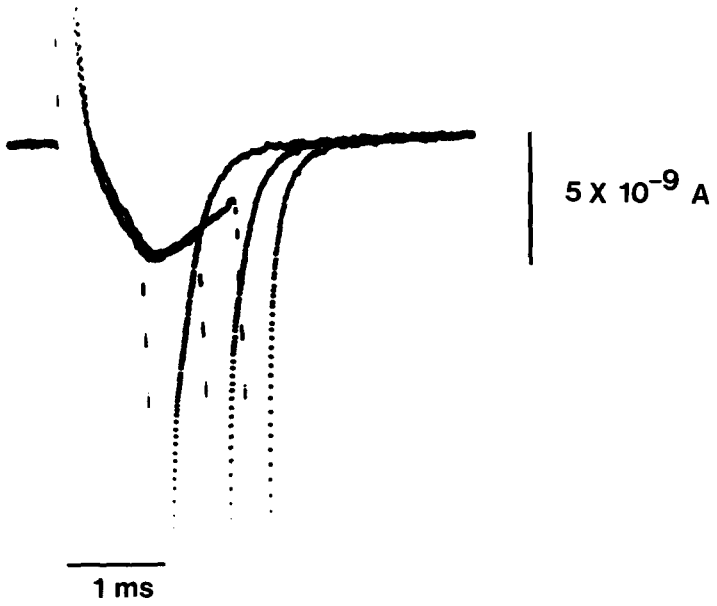

FIGURE 8. Test of voltage control during peak i_{Na}. Superimposed current records were elicited during voltage-clamp steps from a holding potential of −90 to −30 mV for durations of 0.85, 1.5, and 1.9 ms. Note smooth and rapid decays of i_{cap} which merge into sodium tail currents. R_s compensation was used. Data were replayed from an FM tape recorder operated at a bandwidth of 20 kHz.

exercised, and more favorable conditions (50% $[Na^+]_o$) will be used in future, more quantitative studies.

TTX-insensitive Inward Current

A smaller and slower transient inward current (shown in panel C of Fig. 4) can be recorded in the presence of 3×10^{-5} M TTX, a 1,000-fold higher TTX dose than was shown to reduce i_{Na} by 10-fold (see above). Under these conditions, there is nearly a complete block of i_{Na} by TTX. Our data consistently show that 3×10^{-5} M TTX does not reduce further the magnitude of the residual, or second, inward current (see Fig. 4).

Fig. 9 illustrates a typical series of current records (in the presence of 3×10^{-6} M TTX) elicited by 250-ms depolarizing voltage-clamp steps from the

holding potential (−80 mV = zero current potential). Note that voltage-clamp steps ± 10 mV from the holding potential elicit quasi-instantaneous jumps of steady current which are *not* of equal magnitude. Since the depolarizing voltage-clamp step to −70 mV elicits an apparent instantaneous jump of current which is smaller than that elicited by the hyperpolarizing voltage-clamp step to −90 mV, it appears that the time-independent, background *I-*

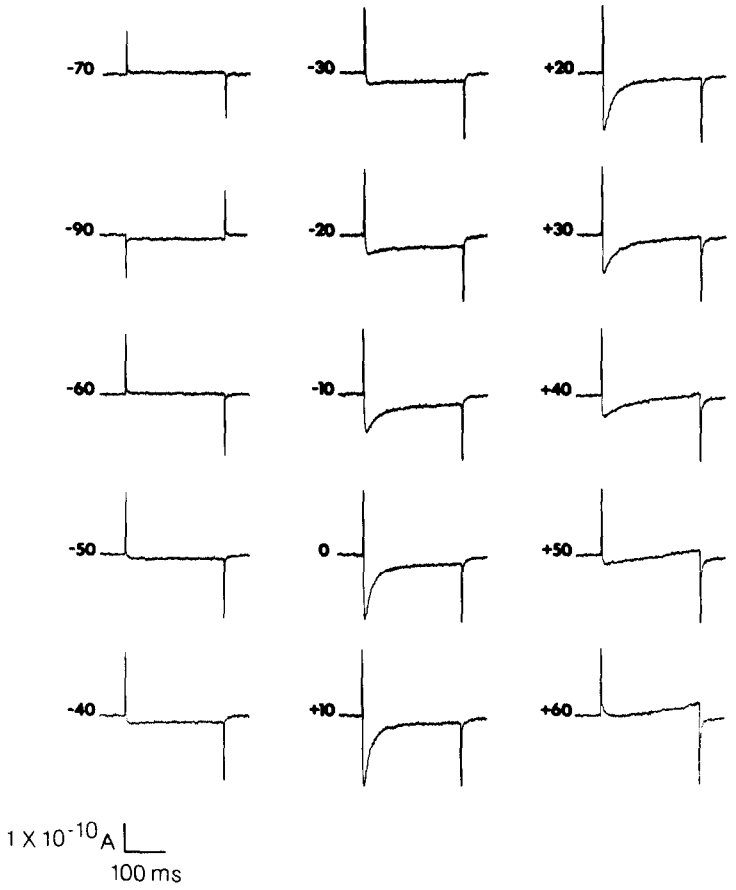

FIGURE 9. TTX-insensitive (3 × 10^{-6} M TTX) ionic currents elicited by voltage-clamp steps (in 10-mV increments) from the holding potential of −80 mV. The numbers to the left of each current trace refer to the level of each voltage-clamp step. Data were displayed on a chart recorder after being recorded on an FM tape recorder at a 5-kHz bandwidth.

V relation is not linear near the resting potential (see *Background Time-independent Current*). A similar phenomenon, attributed to inward-going rectification of a K^+ channel, has previously been observed in voltage-clamp recordings from syncytial cardiac preparations (cf. Noble and Tsien, 1968).

Voltage-clamp steps to progressively more positive potentials (−50 to −40 mV) elicit a small inward current which turns on and remains activated for

the duration of the 250-ms pulse. The failure to inactivate completely is somewhat surprising. This region of the *I-V* relation of most multicellular cardiac preparations has been reported to be dominated by an inwardly rectifying time-independent *outward* current, i_{k_1}, (Noble, 1965; McAllister and Noble, 1966; Noble, 1979). Since in atrial cells having normal resting potentials this small *inward* component may persist for seconds, we will refer to it as a TTX-insensitive, persistent inward current.

Larger depolarizations elicit a transient inward current with an apparent threshold near −30 mV. A striking difference between this transient current and the slow inward current, i_{si}, which has been previously studied in a variety of other cardiac preparations, is its very rapid onset, or speed of activation (4–7 ms time to peak at +10 mV; see also Fig. 4). In response to moderate depolarizations, this transient inward current declines to a steady level which, however, is still inward. As shown in Fig. 9, the transient inward current peaks between 0 and +10 mV, at a magnitude of $\sim 2.5 \times 10^{-10}$ A, and exhibits an apparent reversal potential near +60 mV. Depolarizations to +20 mV or beyond cause the late current (measured at the end of a 250-ms pulse) to become outward (see *Time-dependent Outward Current*).

As previously discussed, the use of a single suction microelectrode for measuring potential and injecting current simultaneously is not expected to produce a significant distortion of the time course or voltage dependence of the TTX-insensitive transient inward current, since its peak magnitude is very small. This supposition can be tested empirically by comparing the *I-V* relations of the TTX-insensitive inward current measured (*a*) with a single suction microelectrode and (*b*) with two microelectrodes, one to measure potential and one to inject current. These *I-V* relations are shown in Fig. 10. The data from the single suction microelectrode experiments represent the mean values of the peak inward and late (250 ms) currents recorded in eight different cells. The data for the two-microelectrode experiments represent mean values of the peak inward and late (250 ms) currents recorded in three different cells. It is apparent that very similar results are obtained by the two methods: the voltage dependence and peak magnitude of the TTX-insensitive transient inward current agree within experimental error. The mean peak amplitude of TTX-insensitive current recorded in eight cells using a single-micropipette voltage clamp corresponds to a peak inward current density of $\sim 9 \times 10^{-6}$ A/cm^2.

As noted previously in the description of i_{Na}, it is possible to assess the degree to which the single cell is space-clamped during activation of $i_{Ca^{++}}$. In Fig. 10, the maximum slope conductance in the range of potentials positive to 0 mV is 156 MΩ. When compared with the R_{IN} of the single electrode data (Table I: 284 MΩ), this suggests that the DC space constant of the quiescent cell (~1,008 μm) will be reduced by a factor of 1.35 during activation of $i_{Ca^{++}}$. Note, however, that this reduction still gives a "space constant" of 747 μm, or about three times the length of a single atrial cell.

There are two definite advantages of using a single suction microelectrode rather than two conventional microelectrodes: (*a*) a single-electrode impalement is easier to obtain and hold, and (*b*) it has the ability to achieve a very

high seal resistance. Both of these dramatically reduce the magnitude of leak current artefacts that arise from incomplete sealing around microelectrodes. This series of voltage-clamp protocols was performed only on single cells in which a high shunt resistance was established by the suction microelectrodes, i.e., those that exhibit quiescent resting potentials between −80 and −90 mV. In each experiment, the myocyte was initially clamped to a holding potential very close to its resting or zero-current potential. Care was taken to correct for

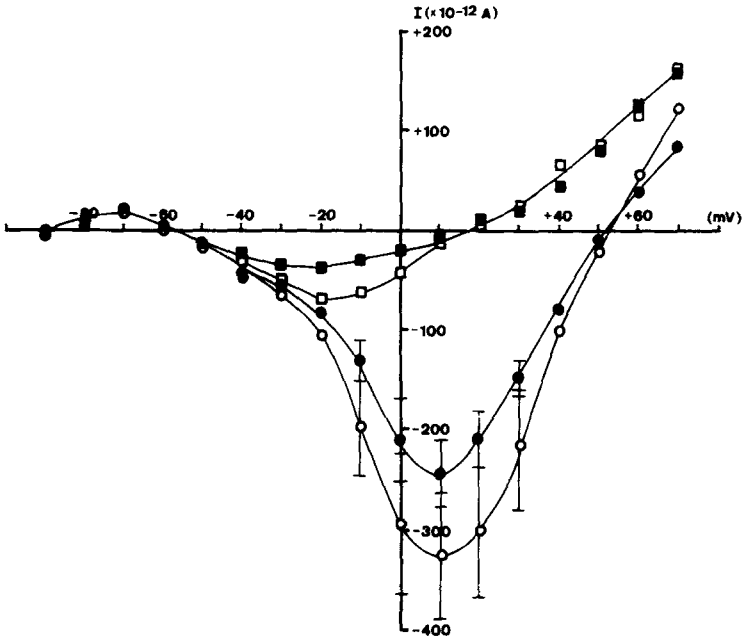

FIGURE 10. Peak inward current (circles) and late current (squares; measured at the end of 250 ms) recorded in the presence of 3×10^{-6} M TTX and $[Ca^{++}]_o$ 2.5×10^{-3} M. The peak inward, or minimum outward, current was measured with reference to the zero current level, since in all cases the holding potential was set close to the resting potential. No leakage correction procedures were used. The filled symbols represent mean values for eight cells obtained with the single suction microelectrode voltage clamp. The open symbols represent mean values for three cells and were obtained using a conventional two-microelectrode voltage clamp. Vertical bars denote standard errors. Note that (*a*) there are no significant differences between the data obtained using these two voltage-clamp methods, and (*b*) a persistent inward current remains at the end of the 250-ms pulse in the range (−60 to +10 mV).

small changes in tip potentials (only electrodes with tip potentials <5 mV were used), and the stability of zero-current potential was checked at the end of each protocol by turning off the clamp and measuring the membrane potential directly. Each current-voltage relation has been plotted with reference to the zero-current potential (e.g., the resting membrane potential).

To further characterize the TTX-resistant transient inward current, we have examined its sensitivity to changes in $[Ca^{++}]_o$ or $[Na^+]_o$, and have applied

agents that block Ca^{++} channels. Fig. 11 illustrates the effects of increasing $[Ca^{++}]_o$ from 2.5 to 7.5 mM in TTX-containing Ringer (3×10^{-6} M). The magnitude of transient inward current recorded at the peak of the *I-V* relation was increased about twofold by increasing $[Ca^{++}]_o$ and the apparent reversal potential was shifted ~10 mV in the depolarizing direction. This is consistent with an increase in driving force in 7.5 mM Ca^{++}, if Ca^{++} is the major permeant cation. Surprisingly, there is little change in the late *I-V* relation measured at 250 ms. In particular, the persistent inward current component is not changed significantly.

The results of experiments such as those shown in Fig. 11 also indicate that the time course of the inactivation of the TTX-resistant transient inward current is modified by changes in $[Ca^{++}]_o$. This may indicate that inactivation of this current is at least partially mediated by a current-dependent process (see Hume and Giles, 1982*a*), as originally described in *Paramecium* (Brehm and Eckert, 1978) and *Aplysia* neurones (Tillotson, 1979). Alternative mechanisms for inactivating the slow inward current in frog atrial trabeculae have previously been described (Horackova and Vassort, 1976; Fischmeister et al., 1981).

In other experiments, $[Ca^{++}]_o$ has been replaced completely by $[Mg^{++}]_o$. As shown in Fig. 12, the TTX-resistant transient inward current disappears completely in this nominally zero $[Ca^{++}]_o$, which further suggests that this current is predominantly a Ca current. The relative insensitivity of the persistent inward current to short-term changes in $[Ca^{++}]_o$ is again observed (for further discussion, see *Background Time-independent Currents*).

Possible contributions to the TTX-insensitive transient inward current either by Na^+ influx through a TTX-insensitive Na^+ channel or by Na^+ influx through the Ca^{++} channel were assessed in a series of experiments in which NaCl was replaced completely by sucrose. Superfusion with Na^+-free Ringers solution produced a rapid contracture of all the cells in the recording chamber; thus, it was impossible to obtain data from the same cell before and after changing to 0 $[Na^+]_o$. Within 15 min in 0-Na^+ Ringers, some cells relaxed, making it possible to establish a giga-seal and perform voltage-clamp protocols. Fig. 13 shows the mean values from three such cells for peak inward and late currents (250 ms) in 0 $[Na^+]_o$ and TTX (3×10^{-6} M). Comparison of Figs. 10 and 13 shows that very little change occurred in (*a*) the amplitude of the peak inward current or (*b*) the apparent reversal potential. Although more extensive studies are required to determine conclusively the extent to which Na^+ influx through Ca^{++} channels contributes to i_{Ca} in single atrial cells; these data suggest that no significant TTX-insensitive Na^+ flux generates either (*a*) the TTX-insensitive transient inward current, $i_{Ca^{++}}$, or (*b*) the persistent inward current.

From the data presented in Figs. 11–13, it would appear that the persistent inward current is uninfluenced by short-term exposure to either nominally 0 $[Na^+]_o$ or 0 $[Ca^{++}]_o$. A possible explanation for this finding is that this current is carried by Ca^{++} and/or Na^+ which is bound to sites on the sarcolemma. Our preliminary data (Hume and Giles, unpublished) indicate that La^{++} (0.1 mM) will block this persistent inward current. Since it is not reduced signifi-

cantly in nominally 0 $[Na^+]_o$, the persistent inward current is unlikely to be generated entirely by an electrogenic Na^+/Ca^{++} exchange mechanism (cf. Mullins, 1979; Chapman, 1979).

A major difficulty in the study of Ca^{++} currents has been an inability to define accurately its reversal potential (for review see Hagiwara and Byerly, 1981). This is primarily due to technical difficulties in the measurement and interpretation of outwardly directed current through Ca channels. Most estimates of a reversal potential for i_{Ca} in multicellular cardiac preparations

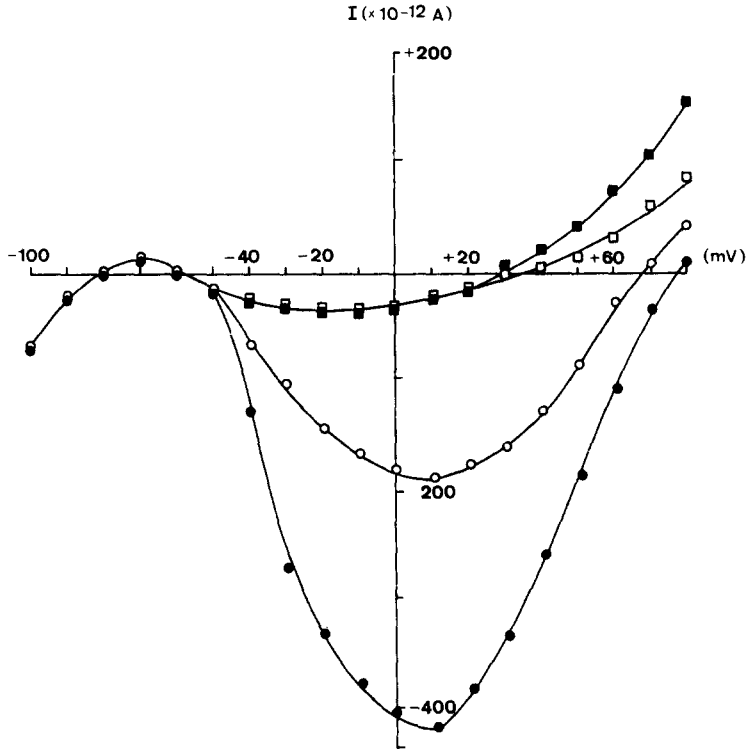

FIGURE 11. Effect of raising $[Ca^{++}]_o$ on the peak inward (circles) and late (squares) current-voltage relation, obtained in 3×10^{-6} M TTX. Data illustrated as open symbols were recorded in 2.5 mM $[Ca^{++}]_o$; filled symbols show data obtained in 7.5 mM $[Ca^{++}]_o$. A single suction microelectrode voltage clamp was used. Holding potential: −80 mV, the zero-current potential.

indicate that E_{rev} is much more negative than the $E_{Ca^{++}}$ calculated from the Nernst equation, if intracellular free Ca^{++} is near 10^{-7} M (Beeler and Reuter, 1970; New and Trautwein, 1972; McDonald and Trautwein, 1978). Possible explanations for this observation include Na^+ influx (Rougier et al., 1969) and/or K^+ efflux through Ca^{++} channels (Reuter and Scholz, 1977). Our results indicate an apparent E_{rev} near +50 to +60 mV (see Fig. 10), although these data have not been corrected for leakage currents. An interesting finding regarding the reversal of I_{Ca} is shown in Fig. 14. Voltage-clamp steps positive

to its reversal potential (approximately +60 mV) consistently elicit outward currents that relax with a time course similar to that observed for inwardly directed i_{Ca} at certain more negative potentials. These current records may illustrate an actual reversal of i_{Ca} since both the inward and outward currents are blocked by Ca^{++} antagonists. Future experiments will focus on determining whether this transient outward current is due to either Ca^{++} efflux or K^+ efflux through Ca channels (cf. Lee and Tsien, 1982).

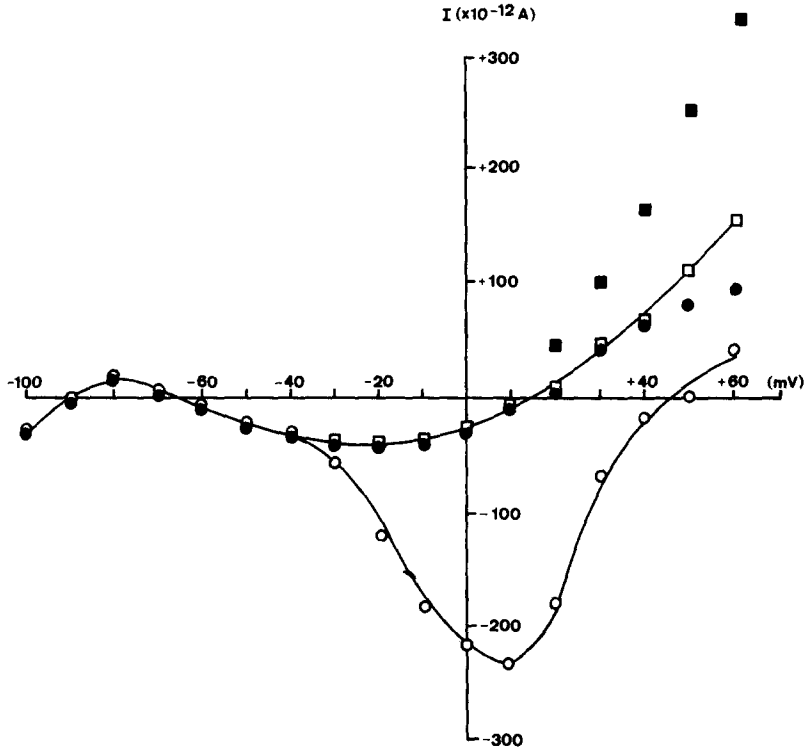

FIGURE 12. Peak inward and late current-voltage relation in 3×10^{-6} M TTX and 2.5 mM $CaCl_2$ (open symbols) and 10 min after equimolar substitution of $CaCl_2$ by $MgCl_2$ (filled symbols), i.e., nominally 0 mM $CaCl_2$. The total divalent cation concentration was constant. Circles are peak inward or minimal outward current, and squares are late current measured at the end of the 250-ms command pulse.

The influence of Ca^{++}-channel antagonists on the TTX-resistant inward current in single atrial cells has been studied qualitatively. In Fig. 15, the effects of 10^{-3} M $CdCl_2$ are shown. Cd^{++} produces a substantial block of the transient inward current. Note, however, that the late currents (in particular the TTX-insensitive persistent inward current) are not changed significantly. Cd^{++} has been shown to be an effective blocker of Ca^{++} channels in a variety of excitable tissues (Adams, 1980; Kostyuk, 1980; Fox and Krasne, 1981) and to have little direct effect on K^+ currents in the node of Ranvier (Århem,

1980). The block we observe is not likely to be due to a surface charge effect, since divalent cation concentration was kept constant by equimolar substitution of Mg^{++}. D-600 and Ni^{++} also block the transient inward current in atrial cells; however, Cd^{++} appears to be more selective. From the *I-V* relation it appears that a small change in E_{rev} may have occurred. However, since the currents are not leakage corrected, a decrease in i_{Ca} in the presence of a steady background leak current could change the apparent reversal potential. For instance, in squid giant axon TTX has been shown to produce an apparent shift in E_{Na} merely by reducing the magnitude of i_{Na} relative to steady state background currents in (Moore et al., 1967).

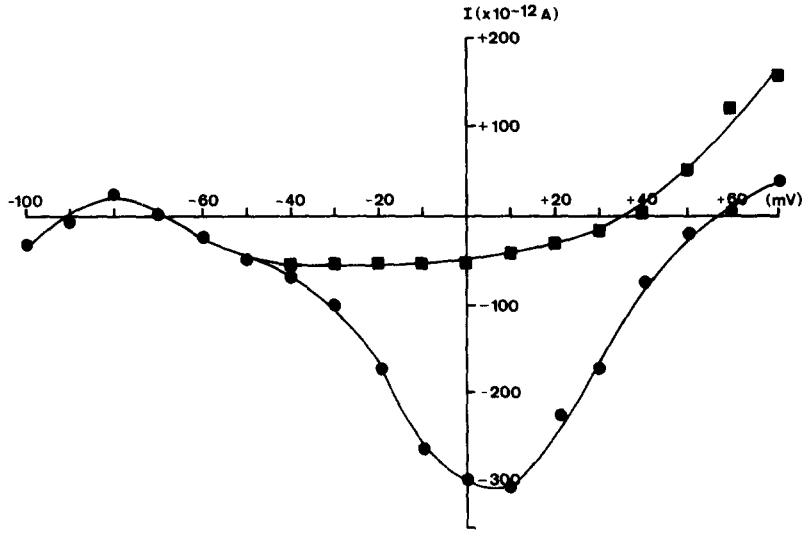

FIGURE 13. Peak inward and late current-voltage relation in nominally Na-free Ringers containing 3×10^{-6} M TTX. Circles indicate the mean peak inward or minimal outward current and squares show the mean late current measured at 250 ms ($n = 3$). Data were obtained ~15 min after switching to Na-free Ringers solution (see text for details).

Time-dependent Outward Current

The outward current(s) has been studied extensively in intact frog atrial trabeculae. However, considerable disagreement exists regarding the number of currents, their activation ranges, and their time dependence (DeHemptinne, 1971; Ojéda and Rougier, 1974; Brown et al., 1976; see Carmeliet and Vereecke, 1979, for review). It was therefore of interest to examine the outward current(s) in single atrial cells. Our initial experiments were carried out to determine whether (*a*) a slow outward current could consistently be recorded, (*b*) one or more than one Hodgkin-Huxley conductance component was required to describe the data, and (*c*) the current was carried mainly by K^+. Fig. 16 shows the results of an experiment aimed at characterizing the slow outward current. The voltage was stepped to +20 mV for 500 ms from a holding potential of −90 mV (zero-current potential for this cell), followed by

600-ms voltage-clamp steps back to −70, −95, and −110 mV (tails photographically superimposed). The first or conditioning voltage-clamp step to +20 mV elicits both inward and outward currents. The TTX-resistant transient inward current activates and then turns off within 100 ms. This is

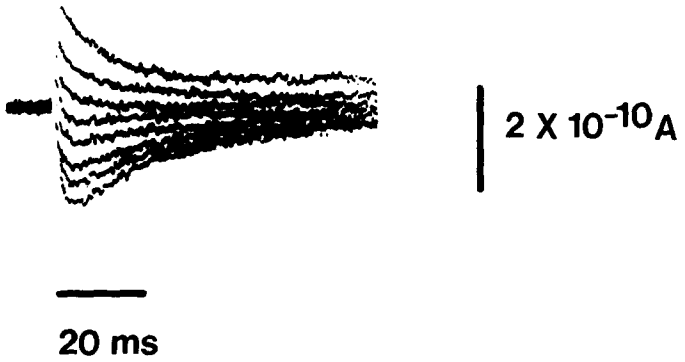

FIGURE 14. Apparent reversal of i_{Ca} transient currents. Superimposed i_{Ca} records were elicited by voltage-clamp depolarizations from +20 to +90 mV in 10-mV increments. Holding potential: −85 mV, the zero-current potential. The apparent E_{rev} occurs between +60 and +70 in this experiment (2.5 mM $[Ca^{++}]_o$).

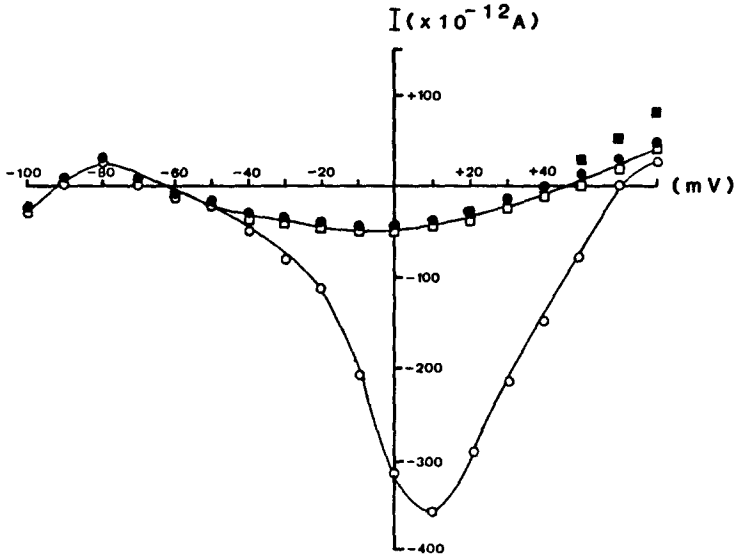

FIGURE 15. Effect of 1×10^{-3} M $CdCl_2$ on peak inward (circles) and late (squares) current-voltage relations obtained in the presence of 3×10^{-6} M TTX. Open symbols show data obtained before and closed symbols indicate data recorded 10 min after the addition of 1×10^{-3} M $CdCl_2$. The single suction microelectrode voltage-clamp method was used. This Cd^{++} dose produces a marked inhibition of the TTX-resistant transient inward current, but has no detectable blocking action on the persistent inward current. Holding potential: −90 mV.

followed by the apparently sigmoid activation of an outward current. The second or test voltage step back to −70 mV results in a outward tail that declines with a single exponential time course. Additional current records for such paired-pulse experiments have been superimposed photographically. When the test voltage-clamp step is to −95 mV, no tail current is recorded; however, if the test step is to −110 mV, a slow inward tail is observed. In six additional experiments in 2.5 $[K^+]_o$, this slow outward current reversed between −95 to −100 mV, which suggests that it is carried mainly by K^+.

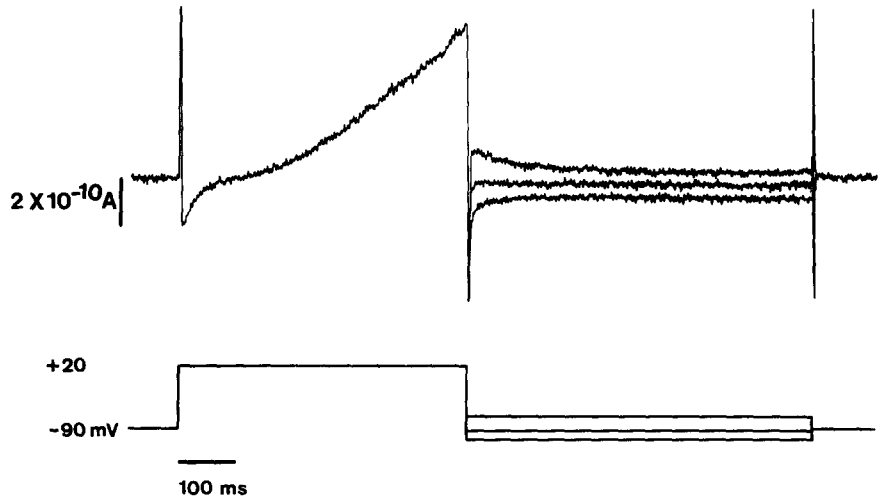

FIGURE 16. Activation and reversal potential of the slow outward current in an isolated single atrial cell. This experiment was done in the presence of TTX (3×10^{-6} M) using the single suction microelectrode voltage clamp. Holding potential: −90 mV. The current and voltage records were made by photographic superposition after being displayed on a chart recorder. The first or conditioning pulse was to +20 mV for 500 ms. The second or test clamp steps were to potentials of −70, −95, and −105 mV. The reversal potential is near −95 mV.

This outward current is consistently observed in single bullfrog atrial cells. Experiments such as the one illustrated in Fig. 16 indicate that during the time course of an action potential (~500 ms), the K^+ current is not significantly influenced by K^+ accumulation. It may seem that the problem of K^+ accumulation could be avoided completely in single myocytes. However, the caveolae and/or the T system (in the case of ventricular cells) may form restricted compartments and increase the likelihood of accumulation/depletion phenomena, which might then modulate the slow outward current. Fig. 17 shows the results of an additional experiment in which longer prepulses were used and a considerably larger K^+ current was activated. In panel A, a 1-s voltage step to +45 mV elicits ~8.0×10^{-10} A of time-dependent outward current. The superimposed tail current records again show that E_{rev} is near −95 mV. If the prepulse voltage step to +45 mV is lengthened to 2 s, ~10^{-9}

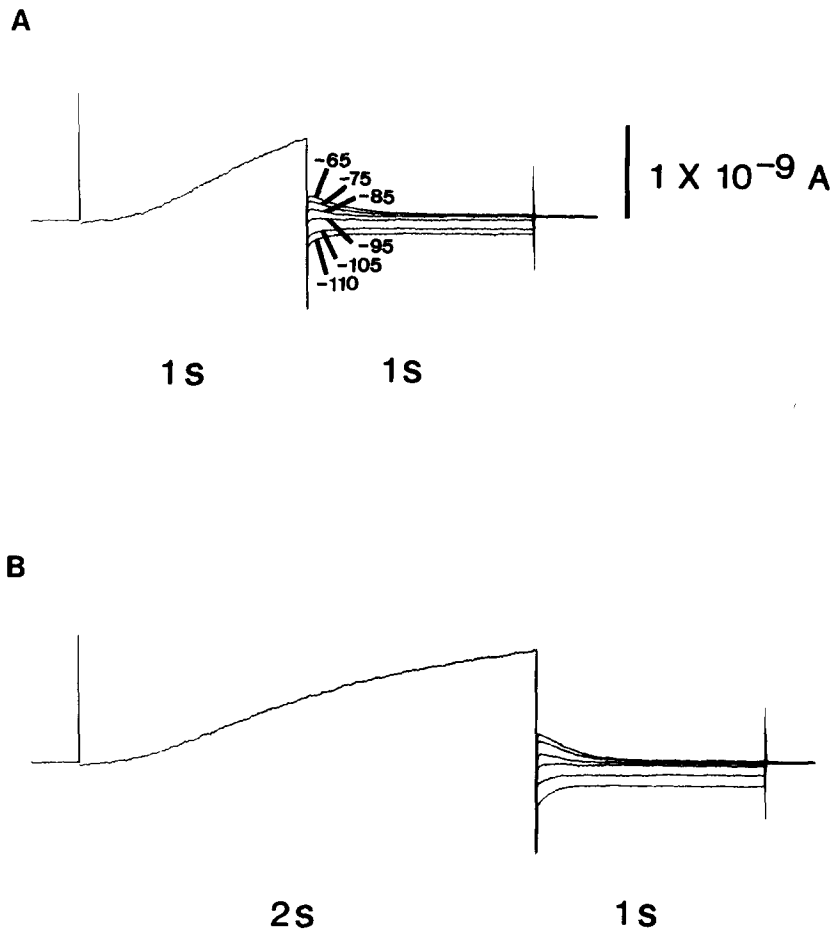

FIGURE 17. Activation and reversal of the slow outward current elicited by long depolarizing clamp steps. These experiments were carried out in the presence of TTX (3×10^{-6} M), using the single suction micropipette voltage clamp. Holding potential: −90 mV. The outward current was activated by repetitive application of a 1-s (panel A) or 2-s (panel B) conditioning pulse to +45 mV, applied at a frequency of 0.2 Hz. The reversal potential was determined by following the conditioning pulse with a 1-s test pulse to the potentials shown in panel A. The same test potentials were applied in panel B, with the exception that the most negative potential was to −115 mV as opposed to −110 mV. The current tails were photographically superimposed. Note that the reversal potential remains fixed near −95 mV after conditioning pulses of either 1 or 2 s.

A of outward current is activated, but E_{rev} remains near −95 mV. In Fig. 18, the tails produced by the repolarizations to −65 mV for both 1- and 2-s depolarizations are shown at a higher gain (panel A). Their time course of decay is plotted in panel B. Both tails decay with the same single exponential

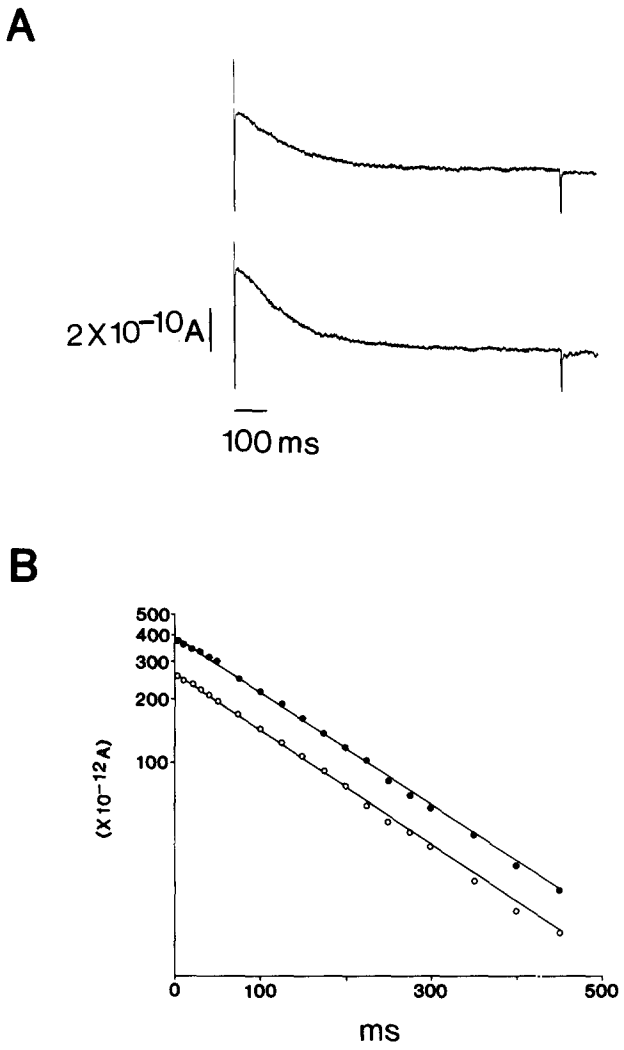

FIGURE 18. Kinetics of decay of outward tail currents. Panel A shows high gain tails of outward current recorded at −65 mV after 1- and 2-s rectangular depolarizing pulses to +45 mV. In panel B, the time course of decay of these tails with respect to the baseline ($I = 0$, holding current) is plotted in log Δi vs. time coordinates. The decay of both tails is well fitted by a single exponential time course (τ = 160 ms). Note that the time constant of decay is independent of the amplitude of the tail currents.

time course. Thus, the rate of decay does not appear to be dependent upon the amount of i_K activated by the prepulse. This observation rules out any significant contribution of accumulation of $[K^+]$ to either the magnitude or the kinetics of i_K recorded in single atrial cells in response to a 2-s depolarization. Thus, it is very unlikely that this K^+ current, which causes repolarization of the action potential, produces a change in the electrochemical

potential for K^+ in our experimental conditions. Furthermore, these data suggest that the slow outward K^+ current in bullfrog atrial cells is adequately described as a single Hodgkin-Huxley process.

Background Time-independent Current

In Figs. 12 and 15 it was shown that in the presence of TTX (3 μm) and after short-term exposure to either nominally 0 $[Ca^{++}]_o$ or Cd^{++} (1 mM), a small persistent inward current remains. The presence of this current precludes accurate measurement of the background time-independent (leak) current-voltage relationship in single frog atrial cells. Because of the importance of defining the background current-voltage relationship for the quantitative measurement of the time-dependent ionic currents, we have further attempted to separate the persistent inward current from the time-independent background current(s). In these studies, atrial cells were superfused with nominally 0 $[Ca^{++}]_o$ Ringers or Cd^{++} (1 mM) for relatively long periods.

Fig. 19 shows the results obtained from a cell that had been bathed in 3 μM TTX and 1 mM Cd^{++} for ~1 h. This pretreatment eliminates the persistent inward current, and the only remaining time-dependent ionic current is the outward K^+ current, which turns on after a considerable delay (see Fig. 19, inset). Under these conditions, the background current-voltage relationship can be obtained by measuring quasi-instantaneous current changes 10 ms after the initiation of depolarizing or hyperpolarizing voltage-clamp steps.

In 2.5 mM $[K^+]_o$, the background current-voltage relation exhibits marked inward-going (anomalous) rectification at potentials positive to the holding potential (−90 mV). Therefore, in 2.5 mM $[K^+]_o$ the time-independent background current is exceedingly small. When $[K^+]_o$ is elevated to 5.0 and 10.0 mM, larger outward currents are elicited by depolarizing clamp steps positive to −70 mV. The resulting time-independent background current-voltage relationships cross over, a phenomenon that has previously been observed in multicellular cardiac preparations, skeletal muscle, and egg cell membranes (for review see Hagiwara and Jaffe, 1979; Hille and Schwarz, 1978). This cross-over effect is a characteristic feature of an inwardly rectifying K^+ channel.

The data in Fig. 19 indicate that there is nearly complete absence of a negative slope in the background current-voltage relation. It is important to remember, however, that at potentials positive to 0 mV these *I-V* curves must include a contribution from the leakage current around the electrode. For example, if this leak pathway is nonspecific (E_{rev} near 0 mV) and the seal resistance is 2×10^9 Ω, at +50 mV this outward leakage current will be 2.5×10^{-11} A, which could effectively hide any negative slope in the inwardly rectifying background current.

DISCUSSION

Suction Micropipette Technique

A hybrid suction micropipette technique has been developed and used to impale long, thin, single cells isolated from the bullfrog atrium. This suction

microelectrode method has been shown to provide reliable electrophysiological measurements in these small isolated cells; the results obtained are very similar to data recorded using conventional microelectrode techniques (Table I). Accurate transmembrane potential measurements can be made using this

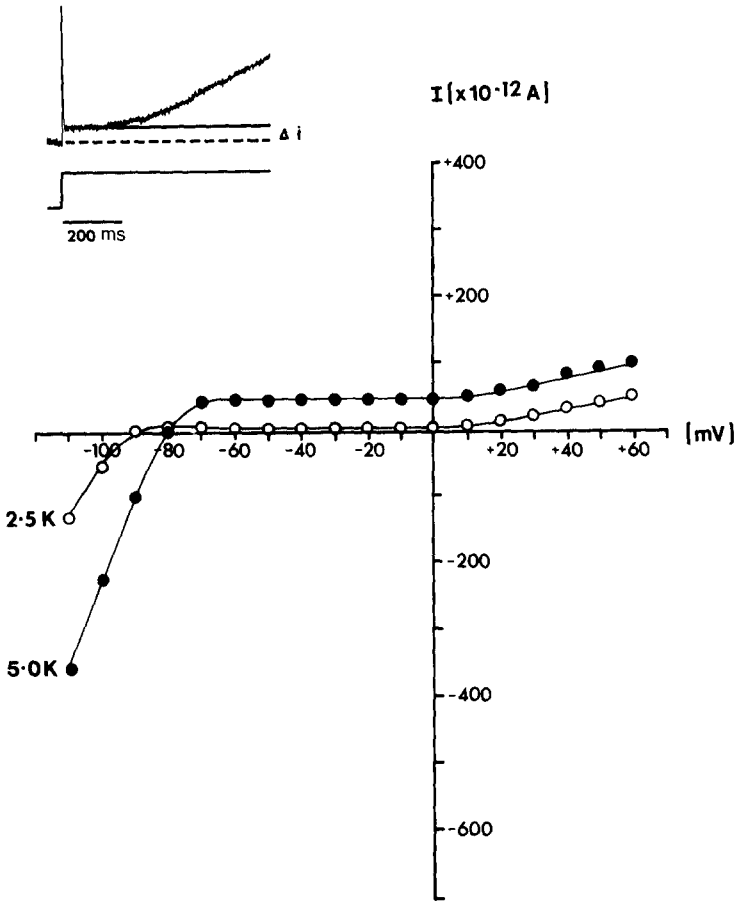

FIGURE 19. Time-independent background current in a single cell from bullfrog atrium. The background current was pharmacologically isolated by blocking the two transient inward currents, as well as the persistent inward current (3 μM TTX and 1 mM Cd^{++} for 60 min). Its quasi-instantaneous *I-V* was measured 10 ms after the start of the command voltage step in 2.5 $[K^+]_o$, shown as (○). Note that this *I-V* relation exhibits marked inward-going rectification. The solid symbols illustrate *I-V* curves obtained after $[K^+]_o$ had been increased to 5. Note that the cross-over phenomenon is observed. See text for further explanation.

suction microelectrode because very large seal resistances (several gigohms) can be established. Moreover, as noted in Methods, the application of a constant negative pressure to the shank of the microelectrode minimizes the loss of the electrolyte (3 M KCl) into the cell. Since this technique permits intracellular impalements with low-resistance microelectrodes and since the

absolute magnitude of the ionic currents in single atrial cells is small, it is possible to use a single microelectrode for injecting current and monitoring the transmembrane potential simultaneously in a voltage-clamp circuit. Hamill et al. (1981) have recently described a single-microelectrode technique for voltage-clamping isolated excitable cells. Their approach is similar in principle to the voltage-clamp method used in our experiments.

The ability to use a single low-resistance microelectrode to voltage-clamp single atrial cells can be evaluated by comparing the results with those obtained using a conventional two-microelectrode technique which has one to inject current and one to monitor voltage. Both methods give similar values for the specific membrane capacitance (obtained from the integral of the capacitative charging currents) of single atrial cells. In addition, very similar current-voltage relations for TTX-insensitive inward current are measured with both techniques. These results suggest that the single-microelectrode voltage-clamp technique is suitable for studying ionic currents of 1×10^{-9} A or less in this preparation, since the voltage error produced by the *I-R* drop across a typical electrode tip (1–2 MΩ) is minimal (1–2 mV). This degree of accuracy in the dynamic measurement of E_m is sufficient for most voltage-clamp protocols. However, series resistance compensation (cf. Hodgkin et al., 1952; Sigworth, 1980; Fishman, 1982) can be used to reduce series resistance artefacts. Utilization of compensated feedback permits larger and/or faster ionic currents, such as i_{Na}, to be studied semi-quantitatively.

The most obvious advantage of the single suction micropipette voltage-clamp technique is the relative ease with which a single-electrode impalement can be made and maintained in a contractile cell. This dramatically increases the success rate of the experiments. Also, the ability to achieve very high seal resistances (several gigohms) ensures that the background (time-independent) currents recorded under voltage-clamp conditions actually reflect properties of the sarcolemma rather than current leaking around the microelectrode tip into the bath. The establishment of high seal resistance also makes it possible to determine very accurately the zero-current potential for each cell (i.e., the resting membrane potential). This is a very important reference level for defining the direction of current changes.

An apparent disadvantage of the use of pipettes with small tip diameter is the inability to effectively perfuse the interior of the cell. This is a significant advantage of other recently developed techniques (Kostyuk et al., 1975; Lee et al., 1980; Hamill et al., 1981; Kostyuk, 1982), since internal application of various blocking agents can be used to separate ionic currents. In future experiments, we intend to "pressure-inject" various substances (e.g., $CsCl_2$ and tetraethylammonium) into single frog atrial cells as a means of separating the different ionic currents. Our present results, however, suggest that the major currents, i_{Na}, i_{Ca}, and i_K, can be separated on the basis of their voltage dependence and kinetics or by using bath-applied blockers.

The Sodium Current i_{Na}

In multicellular cardiac preparations the slow discharge of the membrane capacitance through a resistance in series with the membrane obscures the

onset of i_{Na}. This severely limits quantitative analysis of i_{Na} using conventional voltage-clamp approaches (Colatsky, 1980). The use of a single isolated cell would be expected to minimize this access resistance since endothelial layers of tissue and/or restricted extracellular spaces are removed. This should facilitate the rapid discharge of the membrane capacitance. Nevertheless, when one micropipette is used to voltage-clamp a single atrial cell, the pipette tip itself becomes a significant series resistance and constitutes the limiting factor that determines the rate of discharge of the membrane capacitance. The use of the single-microelectrode clamp to study i_{Na} is also, in principle, limited by the relatively large absolute magnitude of the current. Our results demonstrate, however, that both of these limitations can be minimized by using positive feedback to compensate for the resistance of the electrode. With compensated feedback (*a*) the rate of discharge of the cell capacitance is significantly increased and approaches that expected if the internal resistivity of the cell is the only remaining limiting factor; (*b*) the *I-V* relation of i_{Na} is continuous and symmetrical and its shape and peak are very similar to those measured when the absolute magnitude of i_{Na} is reduced by partially blocking doses of TTX; and (*c*) the kinetics of i_{Na} are comparable to i_{Na} measurements that have been made in isolated rat ventricular cells (Lee et al., 1979; Brown et al., 1981), short rabbit Purkinje fibers (Colatsky and Tsien, 1979*b*) or clusters of embryonic heart cells at 37°C (Ebihara et al., 1980; Ebihara and Johnson, 1980).

i_{Na} data from single atrial cells seem to satisfy many of the criteria commonly used to assess the adequacy of voltage control (Johnson and Lieberman, 1971; Connor et al., 1975; Colatsky and Tsien, 1979*b*). The apparent reversal potential lies between +30 and +40 mV when $[Na]_o = 110$ mM. This is in the range of the calculated equilibrium potential for Na, if $[Na]_i$ lies between 10 (Keenan and Niedergerke, 1967) and 25 mM (Haas et al., 1963). The peak inward current-voltage relation is quite symmetrical and the current traces decay smoothly with no evidence of "abominable notches." Interruption of the activation of i_{Na} near its peak results in smoothly decaying transients, the latter portion of which reflects rapidly declining Na tail currents.

In addition, the size of i_{Na} measured in our experiments seems appropriate for generating the observed dV/dt_{max} of the action potential. Thus, (*a*) using a specific membrane capacity of 2.3 $\mu F/cm^2$ (determined from analysis of capacitative transients), (*b*) a peak i_{Na} amplitude of 5.2×10^{-9} A ($n = 9$) or 68 $\mu A/\mu F$ (measured in single atrial cells), and (*c*) assuming that $I_i = \frac{dV}{dt} C_m$ (specific membrane capacitance), a dV/dt_{max} of the action potential of 30 V/s is predicted. This is similar to the mean value of 42 V/s previously measured in these cells (Hume and Giles, 1981). If the sarcolemmal caveoli increase the total surface area by 50% (cf. Masson-Pevet et al., 1980), then the specific membrane capacitance approaches 1.5 $\mu F/cm^2$ and the predicted dV/dt_{max} of the action potential becomes 45 V/s.

This agreement, however, may be fortuitous. No rigorous checks have yet

been made of the extent of voltage uniformity during the activation of i_{Na}. This calculation assumes that the excitatory response is a membrane action potential (i.e., that no propagation has occurred). Furthermore, the magnitudes of i_{Na} have not been leakage corrected. Therefore, both the peak amplitudes and the apparent E_{rev} may be underestimates. However, contamination of i_{Na} by background current(s) appears to be minimal (see Fig. 19).

The TTX-insensitive Transient Inward Current

The existence of two distinct transient inward currents in single isolated frog atrial cells is supported by three lines of evidence: (*a*) differences in the kinetics of the turn-on and turn-off of the two currents, (*b*) a 30-mV discrepancy in activation ranges, and (*c*) different sensitivities to Na^+ and Ca^{++} replacement and to pharmacological blockers. Our data are therefore consistent with earlier results obtained in intact frog atrial trabeculae (Rougier et al., 1969; Haas et al., 1971; Tarr, 1971; Connor et al., 1975). Our results argue strongly against the possibility that this second transient inward current is an artefact produced by voltage inhomogeneity arising from a large extracellular series resistance (cf. Johnson and Lieberman, 1971). Moreover, it is unlikely that the second inward current is merely a small component of i_{Na} that remains in the presence of 30 μM TTX. i_{Na} in single isolated frog atrial cells is highly sensitive to TTX. Tanaka and Barr (1982) have reported a K_D of $\sim 10^{-8}$ M for saxitoxin, measured from [^{3}H]STX binding in amphibian myocardium. Our data confirms this high sensitivity (Fig. 7), and in addition, it shows that the second inward current remains even in nominally Na^+-free ($\sim$2 mM) Ringers solution.

The voltage dependence and pharmacological properties of the transient inward current recorded in the presence of TTX suggest that this current is somewhat similar to the slow inward (Na^+/Ca^{++}) current, i_{si}, which has been studied in a variety of syncytial cardiac preparations. However, the time to peak of this current in single isolated atrial cells at room temperature is 4–7 ms at +10 mV. This is 10–20 times faster than that of i_{si} recorded in intact atrial trabeculae using a double-sucrose-gap voltage clamp (for comparison see Noble and Shimoni, 1981*a*, *b*). This discrepancy might be attributed to the relatively low access resistance in a single cell preparation since intercellular clefts and endothelial cell layers are absent. Very rapid turn-on kinetics of the slow inward current have also recently been reported in calf Purkinje fibers using a three-microelectrode voltage-clamp technique (Kass et al., 1979), although these data are not directly comparable, because of a temperature difference (37°C). Our results do, however, differ substantially from recent voltage-clamp measurements of i_{si} in isolated rat ventricular myocytes. Thus, Isenberg and Klöckner (1980) report considerably slower turn-on kinetics of i_{si}, even at 37°C. In addition, they find peak currents (when $[Ca^{++}]_o$ is 3.6 mM) an order of magnitude larger than those reported here. Surface area estimates of rat ventricular myocytes (Page and McCallister, 1973; Powell et al., 1980) are only about twofold greater than the apparent surface area of frog atrial cell, but mammalian ventricular cells have an extensive transverse

tubule system. The magnitude of our TTX-resistant transient inward current is much smaller in comparison, but its peak magnitude *is* sufficient to account for the maximum rate of depolarization of the slow response. Thus, assuming that $I_i = \frac{dV}{dt} C_m$ and recalling our measurements of $C_m = 2.3\ \mu F/cm^2$, a peak amplitude of $i_{Ca} = 2.6 \times 10^{-10}$ A ($n = 8$) or 3.4 $\mu A/\mu F$, one would predict a dV/dt_{max} of the slow response of 1.5 V/s. This is similar to the value of 2.2 V/s previously measured (Hume and Giles, 1981). This discrepancy might arise from our surface area estimates being in error because of the presence of caveoli (Page and Niedergerke, 1972; Masson-Pevet et al., 1980). If the caveolae add 50% to the surface area, C_m becomes 1.53 $\mu F/cm^2$ and the dV/dt_{max} of the slow response will be 2.2 V/s. Alternatively, this current might partially turn off during the depolarization phase of the slow response (see Fig. 5), which would increase the disparity. The sodium current in squid axon exhibits this inactivation phenomenon when the rate of depolarization is slowed (Hodgkin and Huxley, 1952). As noted previously, none of our measurements of time-dependent current are corrected for leakage currents. It is interesting that the peak amplitude of i_{Ca} (9 $\mu A/cm^2$) recorded in these experiments is similar to that predicted from earlier voltage-clamp experiments in multicellular cardiac preparations (Reuter, 1979; Kass et al., 1979).

It is important to consider whether the transient TTX-resistant inward current that is measured in the range −10 to +10 mV can trigger contraction. The isolated atrial cells contract and relax in a phasic fashion when repetitively depolarized into the plateau range of potentials. Estimation by integration of the amount of charge entering the cell in response to a 250-ms depolarization from −85 to +10 mV, combined with the assumptions that (*a*) the charge is carried only by Ca^{++}, (*b*) it is distributed uniformly within the entire right cylinder, and (*c*) there is no significant efflux or sequestration for the first 75 ms, yield a total $[Ca^{++}]_i$ of $\sim 1 \times 10^{-5}$ M. Since a $[Ca^{++}]_i$ of $\sim 5 \times 10^{-6}$ M fully activates the contractile proteins, this current can trigger contraction, although it must be remembered that noncontractile protein intracellular Ca^{++} binding sites may be significant "sinks" in these and other cardiac cells.

A second functionally important factor is obvious from the time course of this transient TTX-resistant inward current. Because at 0 mV this current decays or shuts off completely within 100 ms, its turn-off is very unlikely to be importantly involved in repolarization. Moreover, it will be very small ~125 ms after the upstroke; thus, it cannot be responsible for the 300–500-ms plateau that is characteristic of the bullfrog atrial action potential.

The Persistent Inward Current Component

An important new observation in this study is the absence of large outward instantaneous current jumps or displacements in response to depolarizing voltage-clamp steps of ≥20 mV from the holding potential. Such instantaneous current jumps are usually observed in voltage-clamp experiments using standard microelectrode techniques or sucrose gap methods. They have been

considered to represent a genuine time-independent background current (McAllister and Noble, 1966; DeHemptinne, 1971; Noble, 1979).

The single suction microelectrode technique substantially reduces the magnitude of current leakage around the microelectrode tip during current injection since large seal resistances (several gigohms) are established. As a result, such instantaneous outward jumps of current are not observed unless extremely large depolarizations from the zero-current potential are applied or relatively low seal resistances have been established. In our preparations, such instantaneous jumps of outward current immediately after depolarizing voltage-clamp steps reflect a component of linear "leak" current (not a property of the membrane), which is superimposed upon a background current through the sarcolemma (cf. McAllister and Noble, 1966; McAllister et al., 1975).

When large seal resistances are established, an important property of the background steady state current-voltage relation of the single isolated atrial cell is revealed. In the region where an inwardly rectifying outward K current has previously been described (DeHemptinne, 1971; Noble, 1976), we consistently find a region of steady net inward current. This is produced by a small inward current which fails to turn off (at least for ~10 s). The existence of this persistent inward current does not exclude the simultaneous presence of an inwardly rectifying background K current. It is important to note, however, that this steady net *inward* current in this range of potentials must contribute substantially to the action potential plateau. Furthermore, it may be an important determinant of induced pacemaker phenomena.

Some evidence for an analogous steady inward current component in the plateau range of potentials may be found in previous voltage-clamp data from multicellular cardiac preparations. A steady inward current has been described in sheep Purkinje fibers (Dudel et al., 1967). More recent voltage-clamp experiments in multicellular cardiac preparations have confirmed this finding and suggested that it may arise from incomplete inactivation of i_{si} (Reuter, 1973; Trautwein et al., 1975; Gibbons and Fozzard, 1975; Kass and Tsien, 1975; Marban, 1981), or from incomplete inactivation of i_{Na} (Attwell et al., 1979; Colatsky and Gadsby, 1980).

The existence of persistent inward current has also been an essential feature of models attempting to reconstruct the characteristic long plateau of cardiac action potentials. In Noble's 1962 model, such a persistent inward current was simulated by assuming that a small component of g_{Na} was time independent. In later reconstruction models for the Purkinje fiber (McAllister et al., 1975) and for ventricular myocardium (Beeler and Reuter, 1977), both a residual i_{Na} and i_{si} were used to generate the long plateau phase of the action potential and to produce induced pacemaker activity. In retrospect, therefore, it is not surprising that the steady state background current-voltage relation in a single atrial cell has a region of persistent inward current beginning near −60 mV and extending up to at least +10 mV. Such a property is not only compatible with, but may be necessary for, the long plateau phase of the action potential, as well as the phenomenon of "induced" pacing, which can be observed in these single cells (Hume and Giles, 1981).

The ionic nature of this persistent inward current in isolated single atrial cells remains unclear. The voltage range over which it is activated is a complex region of the steady state current-voltage relation. Voltage-clamp evidence suggests that a number of passive ionic currents, as well as an electrogenic Na^+/K^+ pump current, may contribute to the steady state current-voltage relationship (for review see Carmeliet and Vereecke, 1979). In addition, this persistent inward current is difficult to study because its magnitude is quite small (3.0–5.0 × 10^{-10} A). This means that extreme care must be taken to define accurately the zero-current potential of each cell if this current is to be recorded consistently or if semiquantitative comparisons are to be made.

Our preliminary experiments indicate that the persistent inward current is insensitive to changes in either $[Na^+]_o$ or $[Ca^{++}]_o$ (Figs. 12 and 13). Therefore, it is unlikely to be a component of i_{Na} or i_{Ca} that fails to inactivate. As noted in the Results, relatively brief superfusion of a nominally 0-$[Ca^{++}]_o$ solution may not remove Ca^{++} that is bound to the sarcolemma. This remaining bound Ca^{++} may be sufficient to support this persistent inward current. Indeed, longer-term (e.g., 30 min) exposure to nominally 0-$[Ca^{++}]_o$ Ringers or to Cd^{++} (1 mM) does appear to eliminate the persistent inward current (see Fig. 19). It is interesting that a similar persistent inward current has been described in *Helix* neurons (Eckert and Lux, 1975; Akaike et al., 1978) and in vertebrate motoneurons (Schwindt and Crill, 1980), where it has been attributed to an influx of Ca^{++}. An additional possibility is that this current may have some properties in common with the nonselective current responsible for the oscillatory inward current observed after ouabain exposure in Purkinje fibers (Kass et al., 1978) or the nonspecific single-ion-channel currents recently described in cultured rat ventricular myocytes (Colquhoun et al., 1981).

Outward Current(s)

A limiting technical problem in the analysis of outward currents in virtually all syncytial cardiac preparations is the depletion and/or accumulation of K^+ in restricted extracellular spaces. These phenomena may seriously distort the time course of transmembrane current changes and hence invalidate kinetic and reversal potential measurements (Maughan, 1973; Noble, 1976; Attwell et al., 1979; Brown et al., 1980; DiFrancesco and Noble, 1980).

Slow outward currents recorded in the plateau range in Purkinje fibers were originally termed i_{x_1} and i_{x_2} because their apparent reversal potentials were positive to calculated values of E_K. For the same reason, this terminology has been retained in description of outward current(s) in other syncytial cardiac preparations. However, whether the reversal potential for the slow outward current(s) deviates from the expected E_K as a result of K^+ accumulation, or whether the ion transfer mechanism is not highly selective for K^+, is at present highly controversial. In principle, the distinction between these possibilities can be made convincingly in single atrial cells, if the effects of extracellular ion accumulation are minimal.

Our preliminary analysis indicates that only one component of delayed rectification is observed in isolated single atrial cells. The reversal potential of

this current is typically between −95 and −100 mV ($n = 7$). Thus, it reverses very close to E_K. Walker and Ladle (1973) calculated an E_K of −94 ± 0.5 mV, based on ion-sensitive microelectrode data obtained in intact frog atrium when $[K^+]_o = 2.5$ mM. This suggests the slow outward current observed in isolated single atrial cells can be identified as i_K.

Although further experiments are needed to characterize fully this time- and voltage-dependent K^+ current in single atrial cells, our preliminary results suggest that the outward current turns on with a substantial delay, so that it is separated in time from the turn-off of i_{Ca}. In spite of this delay, significant activation of i_K occurs during the time course of an action potential. This current must therefore be involved in initiating repolarization in frog atrium.

The data in Fig. 19 clearly show that the time-independent background *I-V* relation in isolated atrial cells exhibits marked inward-going rectification. In 2.5 $[K^+]_o$ this current reverses near −90 mV, which indicates that it is carried mainly by K ions. The cross-over phenomenon observed when $[K^+]_o$ was increased to 5 mM is characteristic of inwardly rectifying K^+ channels and has been observed previously in trabeculae from amphibian atrium (Noble, 1976) and ventricle (Cleemann, 1981). It is thought that this cross-over provides a basis for the observation that when $[K^+]_o$ is raised, the action potential duration shortens.

Noble and Tsien (1968) observed a similar inwardly rectifying K^+ current, i_{k_1} in sheep Purkinje fibres. They noted that its *I-V* relation exhibited a significant negative slope and suggested that this may be an important determinant of the development of the pacemaker potential. As noted in the Results, our data do not show any convincing negative slope. However, the leakage current around the electrode may obscure this phenomenon.

In any case, the total time-independent background current is very small in healthy, normally polarized atrial cells. Functionally, this is very important because it means that there is very little K^+ efflux during the relatively long plateau phase of the atrial action potential. Experimentally, this is also advantageous because the reversal potential of the transient inward currents can be obtained quite accurately without employing leakage correction procedures.

Dr. T. Iwazumi has provided very valuable assistance in the design and construction of the electronic circuitry. Financial support for these experiments was provided by grants to Dr. Giles (National Institutes of Health HL-27454, American Heart Association 81-835), as well as a National Institutes of Health Postdoctoral Fellowship to Dr. Hume. Dr. Giles holds an Established Investigators Award from the American Heart Association.

Received for publication 13 August 1981 and in revised form 14 June 1982.

REFERENCES

Adams, P. R. 1980. The calcium current of a vertebrate neurone. *In* Advances Physiological Science. Vol. 4: Physiology of Excitable Membranes. J. Salanki, editor. Pergamon Press, Budapest. 135–138.

Akaike, N., K. S. Lee, and A. M. Brown. 1978. The calcium current of *Helix* neuron. *J. Gen.*

Physiol. 71:509–531.

Århem, P. 1980. Effects of some heavy metal ions on the ionic currents of myelinated fibres from *Xenopus laevis*. *J. Physiol.* (*Lond.*). 306:219–231.

Attwell, D., and I. Cohen. 1977. The voltage clamp of multicellular preparations. *Prog. Biophys. Mol. Biol.* 31:201–245.

Attwell, D., I. Cohen, D. Eisner, M. Ohba, and C. Ojéda. 1979. The steady state TTX-sensitive ("window") sodium current in cardiac Purkinje fibres. *Pflügers Arch. Eur. J. Physiol.* 379:137–142.

Attwell, D., D. Eisner, and I. Cohen. 1979. Voltage clamp and tracer flux data: effects of a restricted extracellular space. *Q. Rev. Biophys.* 12:213–261.

Baer, M., P. M. Best, and H. Reuter. 1976. Voltage-dependent action of tetrodotoxin in mammalian cardiac muscle. *Nature* (*Lond.*). 263:344–345.

Barr, L., M. Dewey, and W. Berger. 1965. Propagation of action potentials and the structure of the nexus in cardiac muscle. *J. Gen. Physiol.* 48:797–823.

Beeler, G. W., and H. Reuter. 1970. Membrane calcium current in ventricular myocardial fibres. *J. Physiol.* (*Lond.*). 207:191–209.

Beeler, G. W., and H. Reuter. 1977. Reconstruction of the action potential of ventricular myocardial fibres. *J. Physiol.* (*Lond.*). 268:177–210.

Brehm, P., and R. Eckert. 1978. Calcium entry leads to inactivation of calcium currents in *Paramecium*. *Science* (*Wash. DC*). 202:1203–1206.

Brown, A. M., K. S. Lee, and T. Powell. 1981. Sodium current of single rat heart muscle cells. *J. Physiol.* (*Lond.*). 318:479–500.

Brown, H. F., A. Clark, and S. J. Noble. 1976. Analysis of pacemaker and repolarization currents in frog atrial muscle. *J. Physiol.* (*Lond.*). 258:547–577.

Brown, H. F., D. DiFrancesco, D. Noble, and S. Noble. 1980. The contribution of potassium accumulation to outward currents in frog atrium. *J. Physiol.* (*Lond.*). 306:127–149.

Bustamonte, J. O., T. Watanabe, and T. F. McDonald. 1981. Single cells from adult mammalian heart: isolation procedure and preliminary electrophysiological studies. *Can. J. Physiol. Pharmacol.* 59:907–910.

Carmeliet, E., and J. Vereecke. 1979. Electrogenesis of the action potential and automaticity. *In* Handbook of Physiology Section 2: The Cardiovascular System; Vol. I: The Heart. R. M. Berne, N. Sperelakis, and S. Geiger, editors. American Physiological Society, Bethesda. 269–234.

Chapman, R. A. 1979. Excitation-contraction coupling in cardiac muscle. *Prog. Biophys. Mol. Biol.* 35:1–52.

Cleeman, L. 1981. Heart muscle. Intracellular potassium and inward-going rectification. *Biophys. J.* 36:303–310.

Cohen, C. J., B. P. Bean, T. J. Colatsky, and R. W. Tsien. 1981. Tetrodotoxin block of sodium channels in rabbit Purkinje fibers. Interactions between toxin binding and channel gating. *J. Gen. Physiol.* 78:383–411.

Cohen, C. J., T. J. Colatsky, and R. W. Tsien. 1979. Tetrodotoxin block of cardiac sodium channels during repetitive or steady depolarizations in the rabbit. *J. Physiol.* (*Lond.*). 296:70–71P. (Abstr.)

Colatsky, T. J. 1980. Voltage clamp measurements of sodium channel properties in rabbit cardiac Purkinje fibres. *J. Physiol.* (*Lond.*). 305:215–234.

Colatsky, T. J., and D. C. Gadsby. 1980. Is tetrodotoxin block of background sodium channels in canine cardiac Purkinje fibres voltage-dependent? *J. Physiol.* (*Lond.*). 30:20P. (Abstr.)

Colatsky, T. J., and R. W. Tsien. 1979*a*. Electrical properties associated with wide intercellular clefts in rabbit Purkinje fibres. *J. Physiol.* (*Lond.*). 290:227–252.

Colatsky, T. J., and R. W. Tsien. 1979*b*. Sodium channels in rabbit cardiac Purkinje fibres. *Nature (Lond.)*. 278:265–268.

Cole, K. S. 1968. Membranes, Ions and Impulses. University of California Press, Berkeley. 570 pp.

Colquhoun, D., E. Neher, H. Reuter, and C. F. Stevens. 1981. Inward current channels activated by intracellular Ca in cultured cardiac cells. *Nature (Lond.)*. 294:752–754.

Connor, J., L. Barr, and E. Jakobsson. 1975. Electrical characteristics of frog atrial trabeculae in the double sucrose gap. *Biophys. J.* 15:1047–1067.

DeHemptinne, A. 1971. Properties of the outward currents in frog atrial muscle. *Pflügers Arch. Eur. J. Physiol.* 329:321–331.

DiFrancesco, D., and D. Noble. 1980. The time course of potassium current following potassium accumulation in frog atrium: analytical solutions using a linear approximation. *J. Physiol. (Lond.)*. 306:151–173.

Dudel, J., K. Peper, and W. Trautwein. 1967. The effect of tetrodotoxin on the membrane current in cardiac muscle (Purkinje fibers). *Pflügers Arch. Eur. J. Physiol.* 295:213–226.

Ebihara, L., and E. A. Johnson. 1980. Fast sodium current in cardiac muscle. A quantitative description. *Biophys. J.* 32:779–790.

Ebihara, L., S. Norikazu, M. Lieberman, and E. A. Johnson. 1980. The initial inward current in spherical clusters of chick embryonic heart cells. *J. Gen. Physiol.* 75:437–456.

Eckert, R., and H. D. Lux. 1975. A non-inactivating inward current recorded during small depolarizing voltage steps in snail pacemaker neurons. *Brain Res.* 83:486–489.

Fischmeister, R., D. Mentrard, and G. Vassort. 1981. Slow inward current inactivation in frog heart atrium. *J. Physiol. (Lond.)*. 320:27–28P.

Fishman, H. M. 1982. Current and voltage clamp techniques. *In* Techniques in Cellular Physiology. P. F. Baker, editor. Elsevier/North-Holland, Inc., New York. 1–42.

Fox, A. P., and S. Krasne. 1981. Two calcium currents in egg cells. *Biophys. J.* 33:145*a*. (Abstr.)

Fromm, M., and S. G. Schultz. 1981. Some properties of KCl-filled microelectrodes: correlation of potassium "leakage" with tip resistance. *J. Membr. Biol.* 62:239–244.

Gibbons, W. R., and H. A. Fozzard. 1975. Slow inward current and contraction of sheep cardiac Purkinje fibers. *J. Gen. Physiol.* 65:367–384.

Giles, W. R., and J. R. Hume. 1981. Inward current underlying the 'slow response' in single bullfrog atrial cells. *J. Physiol. (Lond.)*. 317:53P. (Abstr.)

Haas, H. G., H. G. Glitsch, and W. Trautwein. 1963. Natrium Fluxe am vorhof des Froschherzens. *Pflügers Arch. Eur. J. Physiol.* 277:36–47.

Haas, H. G., R. Kern, H. M. Einwachter, and M. Tarr. 1971. Kinetics of Na inactivation in frog atria. *Pflügers Arch. Eur. J. Physiol.* 323:141–157.

Hagiwara, S., and L. Byerly. 1981. Calcium channel. *Annu. Rev. Neurosci.* 4:69–125.

Hagiwara, S., and L. A. Jaffe. 1979. Electrical properties of egg cell membranes. *Annu. Rev. Biophy. Bioeng.* 8:385–416.

Hamill, O. P., A. Marty, E. Neher, B. Sakmann, and F. J. Sigworth. 1981. Improved patch clamp techniques for high-resolution current recording from cells and cell-free membrane patches. *Pflügers Arch. Eur. J. Physiol.* 391:85–100.

Harrington, L., and E. A. Johnson. 1973. Voltage clamp of cardiac muscle in a double sucrose gap. A feasibility study. *Biophys. J.* 13:626–647.

Hille, B., and W. Schwarz. 1978. Potassium channels as multi-ion single-file pores. *J. Gen. Physiol.* 72:409–442.

Hodgkin, A. L., and A. F. Huxley. 1952. A quantitative description of membrane current and its application to conduction and excitation in nerve. *J. Physiol. (Lond.)*. 117:500–544.

Hodgkin, A. L., A. F. Huxley, and B. Katz. 1952. Measurement of current-voltage relations in

the membrane of the giant axon of *Loligo*. *J. Physiol.* (*Lond.*). 116:424–448.

Horackova, M., and G. Vassort. 1976. Calcium conductance in relation to contractility in frog myocardium. *J. Physiol.* (*Lond.*). 259:597–616.

Horn, R., and M. Brodwick. 1980. Acetylcholine-induced current in perfused rat myoballs. *J. Gen. Physiol.* 75:297–321.

Hume, J. R., and W. Giles. 1981. Active and passive electrical properties of single bullfrog atrial cells. *J. Gen. Physiol.* 78:18–43.

Hume, J. R., and W. Giles. 1982*a*. Turn-off of a TTX-resistant inward current 'i_{Ca}^{++}' in single bullfrog atrial cells. *Biophys. J.* 37:240. (Abstr.)

Hume, J. R., and W. Giles. 1982*b*. Outward current in single bullfrog atrial cells. *Biophys. J.* 37:239. (Abstr.)

Iijima, T., and A. J. Pappano. 1979. Ontogenetic increase of the maximal rate of rise of the chick embryonic heart action potential. *Circ. Res.* 44:358–367.

Isenberg, G., and N. Klöckner. 1980. Glycocalyx is not required for slow inward current in isolated rat heart myocytes. *Nature* (*Lond.*). 284:358–360.

Jack, J. J. B., D. Noble, and R. W. Tsien. 1975. Electric Current Flow in Excitable Cells. Clarendon Press, Oxford. 502 pp.

Johnson, E. A., and M. Lieberman. 1971. Heart: excitation and contraction. *Annu. Rev. Physiol.* 33:479–532.

Kass, R. S., S. A. Siegelbaum, and R. W. Tsien. 1976. Incomplete inactivation of the slow inward current in cardiac Purkinje fibres. *J. Physiol.* (*Lond.*). 263:127–128P.

Kass, R. S., S. A. Siegelbaum, and R. W. Tsien. 1979. Three-microelectrode voltage clamp experiments in calf cardiac Purkinje fibres: is slow inward current adequately measured? *J. Physiol.* (*Lond.*). 290:201–225.

Kass, R. S., and R. W. Tsien. 1975. Multiple effects of calcium antagonists on plateau currents in cardiac Purkinje fibers. *J. Gen. Physiol.* 66:169–192.

Kass, R. S., R. W. Tsien, and R. Weingart. 1978. Ionic basis of transient inward current induced by strophanthidin in cardiac Purkinje fibres. *J. Physiol.* (*Lond.*). 281:209–226.

Keenan, M. J., and R. Niedergerke. 1967. Intracellular sodium concentration and resting sodium fluxes of the frog heart ventricle. *J. Physiol.* (*Lond.*). 188:235–260.

Kostyuk, P. G. 1980. Calcium ionic channels in electrically excitable membrane. *In* Neuroscience. Pergamon Press, Oxford. 5:945–959.

Kostyuk, P. G. 1982. Intracellular perfusion. *Annu. Rev. Neurosci.* 5:107–120.

Kostyuk, P. G., O. A. Kristal, and V. I. Pidoplichko. 1975. Effect of internal fluoride and phosphate on membrane currents during intracellular dialysis of nerve cells. *Nature* (*Lond.*). 257:691–693.

Lee, K. S., N. Akaike, and A. M. Brown. 1980. The suction pipette method for internal perfusion and voltage clamp of small excitable cells. *J. Neurosci. Methods.* 2:51–78.

Lee, K. S., and R. W. Tsien. 1982. Reversal of current through calcium channels in dialyzed single heart cells. *Nature* (*Lond.*). 297:498–501.

Lee, K. S., T. A. Weeks, R. L. Kao, N. Akaike, and A. M. Brown. 1979. Sodium current in single heart muscle cells. *Nature* (*Lond.*). 278:269–271.

Marban, E. 1981. Inhibition of transient outward current by intracellular ion substitution unmasks slow inward calcium current in cardiac Purkinje fibers. *Pflügers Arch. Eur. J. Physiol.* 39:102–106.

Masson-Pevet, M., D. Gros, and E. Besselson. 1980. The caveolae in rabbit sinus node and atrium. *Cell Tissue Res.* 208:183–196.

Maughan, D. 1973. Some effects of prolonged polarization on membrane currents in bullfrog atrial muscle. *J. Membr. Biol.* 11:331–352.

McAllister, R. E., and D. Noble. 1966. The time and voltage dependence of slow outward current in cardiac Purkinje fibres. *J. Physiol.* (*Lond.*). 186:632–662.

McAllister, R. E., D. Noble, and R. W. Tsien. 1975. Reconstruction of the electrical activity of cardiac Purkinje fibres. *J. Physiol. (Lond.)*. 251:1–59.

McDonald, T. F., and W. Trautwein. 1978. Membrane currents in cat myocardium: separation of inward and outward components. *J. Physiol. (Lond.)*. 274:193–216.

Merickel, M. 1980. Design of a single electrode voltage clamp. *J. Neurosci. Methods*. 3:87–96.

Moore, J. W., M. P. Blaustein, N. C. Anderson, and T. Narahashi. 1967. Basis of tetrodotoxin's selectivity in blockage of squid axons. *J. Gen. Physiol.* 50:1401–1411.

Mullins, L. 1979. The generation of electric currents in cardiac fibres by Na/Ca exchange. *Am. J. Physiol.* 236:C103–C110.

Narahashi, T. 1974. Chemicals as tools in the study of excitable membranes. *Physiol. Rev.* 54:814–889.

Narahashi, T., J. W. Moore, and W. R. Scott. 1964. Tetrodotoxin blockage of sodium conductance increase in lobster giant axons. *J. Gen. Physiol.* 47:965–774.

Nathan, R. D., and R. L. DeHaan. 1979. Voltage-clamp analysis of embryonic heart cell aggegates. *J. Gen. Physiol.* 73:175–198.

Neher, E., B. Sakmann, and J. H. Steinbach. 1978. The extracellular patch clamp: a method for resolving currents through individual open channels in biological membranes. *Pflügers Arch. Eur. J. Physiol.* 375:219–228.

New, W., and W. Trautwein. 1972. The ionic nature of slow inward current and its relation to contraction. *Pflügers Arch. Eur. J. Physiol.* 334:24–38.

Noble, D. 1962. A modification of the Hodgkin-Huxley equations applicable to Purkinje fibre action and pace-maker potentials. *J. Physiol. (Lond.)*. 160:317–352.

Noble, D. 1965. Electrical properties of cardiac muscle attributable to inward-going (anomolous) rectification. *J. Cell. Comp. Physiol.* 66:127–136.

Noble, D. 1979. The Initiation of the Heartbeat. Claredon Press, Oxford, England. 156 pp.

Noble, D., and R. W. Tsien. 1968. The kinetics and rectifier properties of the slow potassium current in cardiac Purkinje fibres. *J. Physiol. (Lond.)*. 195:185–214.

Noble, S. 1976. Potassium accumulation and depletion in frog atrial muscle. *J. Physiol. (Lond.)*. 258:579–613.

Noble, S., and Y. Shimoni. 1981*a*. The calcium and frequency dependence of the calcium current 'staircase' in frog atrium. *J. Physiol. (Lond.)*. 310:57–77.

Noble, S., and Y. Shimoni. 1981*b*. Voltage-dependent potentiation of the slow inward current in frog atrium. *J. Physiol. (Lond.)*. 310:77–97.

Ojéda, C., and O. Rougier. 1974. Kinetic analysis of the delayed outward currents in frog atrium. Existence of two types of preparation. *J. Physiol. (Lond.)*. 239:51–73.

Page E., and L. P. McCallister. 1973. Studies on the intercalated disc of rat left ventricular myocardial cells. *J. Ultrastruct. Res.* 43:388–411.

Page, S. G., and R. Niedergerke. 1972. Structures of physiological interest in the frog heart ventricle. *J. Cell Sci.* 11:179–203.

Powell, T., D. A. Terrar, and V. N. Twist. 1980. Electrical properties of individual cells isolated from adult rat ventricular myocardium. *J. Physiol. (Lond.)*. 302:131–153.

Powell, T., and V. W. Twist. 1976. A rapid technique for the isolation and purification of adult cardiac muscle cells having respiratory control and tolerance to calcium. *Biochem. Biophy. Res. Commun.* 72:327–333.

Reuter, H. 1973. Divalent cations as charge carriers in excitable membranes. *Prog. Biophys. Mol. Biol.* 26:1–43.

Reuter, H. 1979. Properties of two inward membrane currents in the heart. *Annu. Rev. Physiol.* 41:413–424.

Reuter, H., and H. Scholz. 1977. A study of the ion selectivity and the kinetic properties of the calcium dependent slow inward current in mammalian cardiac muscle. *J. Physiol. (Lond.)*. 264:17–47.

Rougier, O., G. Vassort, D. Garnier, Y. M. Gargouil, and E. Coraboeuf. 1969. Existence and role of a slow inward current during the frog atrial action potential. *Pflügers Arch. Eur. J. Physiol.* 308:91–110.

Rougier, O., G. Vassort, and R. Stampfli. 1968. Voltage clamp experiments on frog atrial heart muscle fibres with the sucrose-gap technique. *Pflügers Arch. Eur. J. Physiol.* 301:91–108.

Schoenberg, M., G. Dominquez, and H. A. Fozzard. 1975. Effect of diameter on membrane capacity and conductance of sheep cardiac Purkinje fibers. *J. Gen. Physiol.* 65:441–458.

Schwindt, P. G., and W. E. Crill. 1980. Properties of a persistent inward current in normal and TEA-injected motorneurons. *J. Neurophysiol.* 43:1700–1724.

Sigworth, F. 1980. The variance of the sodium current fluctuations at the node of Ranvier. *J. Physiol. (Lond.).* 307:97–131.

Sommer, J. R., and E. A. Johnson. 1968. Cardiac muscle. A comparative study in Purkinje fibres and ventricular fibres. *J. Cell Biol.* 36:497–526.

Sommer, J. R., and E. A. Johnson. 1969. Cardiac muscle. A comparative ultrastructural study with special reference to frog and chicken hearts. *Z. Zellforsch. Mikrosk. Anat.* 98:437–468.

Tanaka, J., and L. Barr. 1982. Binding of ^{3}H-STX to myocardial sarcolemma from several species. *Biophys. J.* 37:319. (Abstr.)

Tarr, M. 1971. Two inward currents in frog atrial muscle. *J. Gen. Physiol.* 58:523–543.

Tarr, M., and J. W. Trank. 1971. Equivalent circuit of frog atrial tissue as determined by voltage clamp-unclamp experiments. *J. Gen. Physiol.* 58:511–522.

Tarr, M., and J. W. Trank. 1974. An assessment of the double sucrose-gap voltage clamp technique as applied to frog atrial muscle. *Biophys. J.* 14:627–643.

Taylor, R. E., J. W. Moore, and K. S. Cole. 1960. Analysis of certain errors in squid axon voltage clamp measurements. *Biophys. J.* 1:161–202.

Tillotson, D. 1979. Inactivation of Ca conductance dependent on entry of Ca ions in molluscan neurons. *Proc. Natl. Acad. Sci. USA.* 76:1497–1500.

Trautwein, W., T. F. McDonald, and O. Tripathi. 1975. Calcium conductance and tension in mammalian ventricular muscle. *Pflügers Arch. Eur. J. Physiol.* 354:55–74.

Walker, J. L., and R. O. Ladle. 1973. Frog heart intracellular potassium activities measured with potassium microelectrodes. *Am. J. Physiol.* 225:263–267.